Lensing

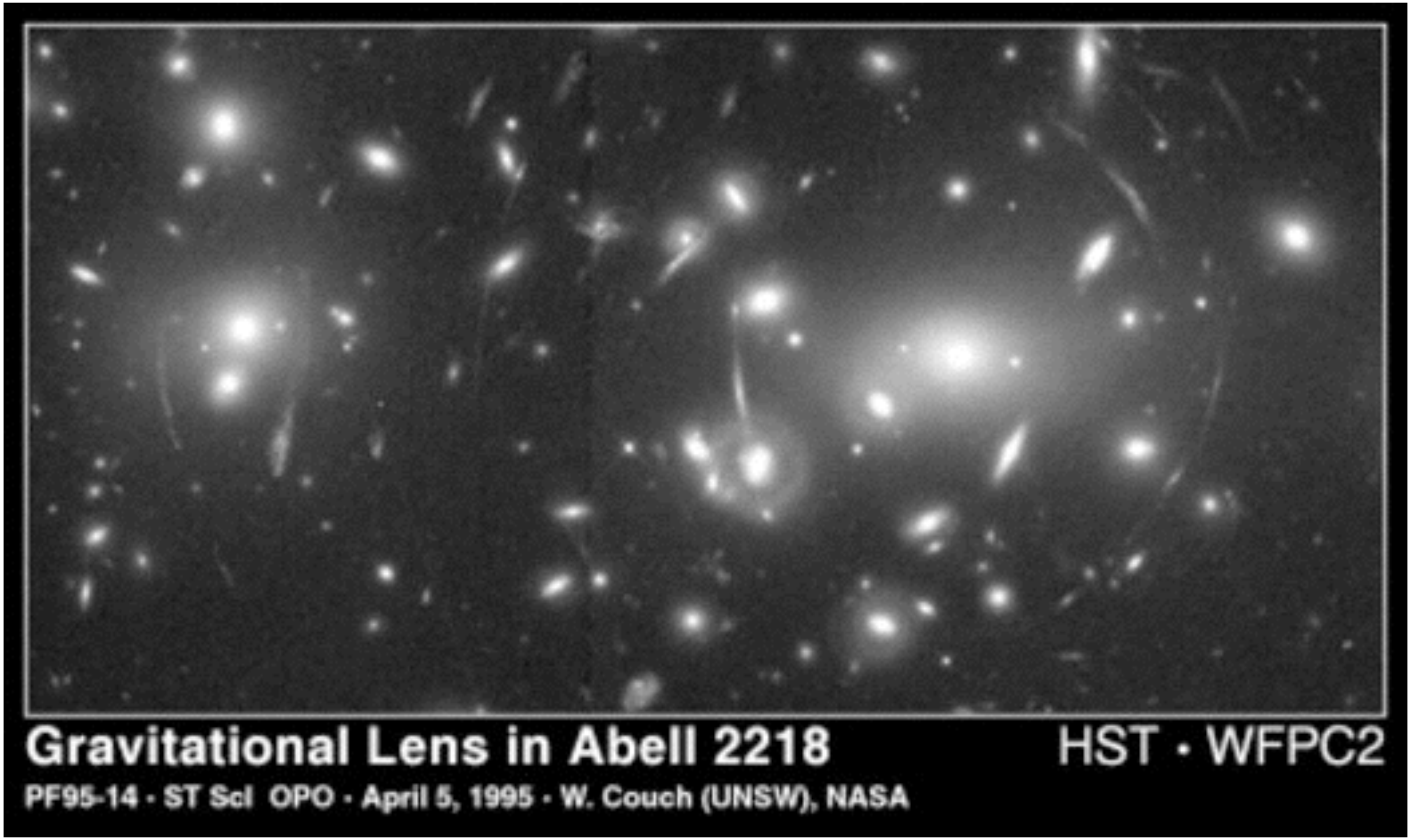
Gravitational Lens in Abell 2218
HST · WFPC2
PF95-14 · ST ScI OPO · April 5, 1995 · W. Couch (UNSW), NASA

Strong lensing: distortion at large angular scales

Microlensing

microlensing: distortion at small angular scales (θ ≈ 1 mas)

Einstein Ring

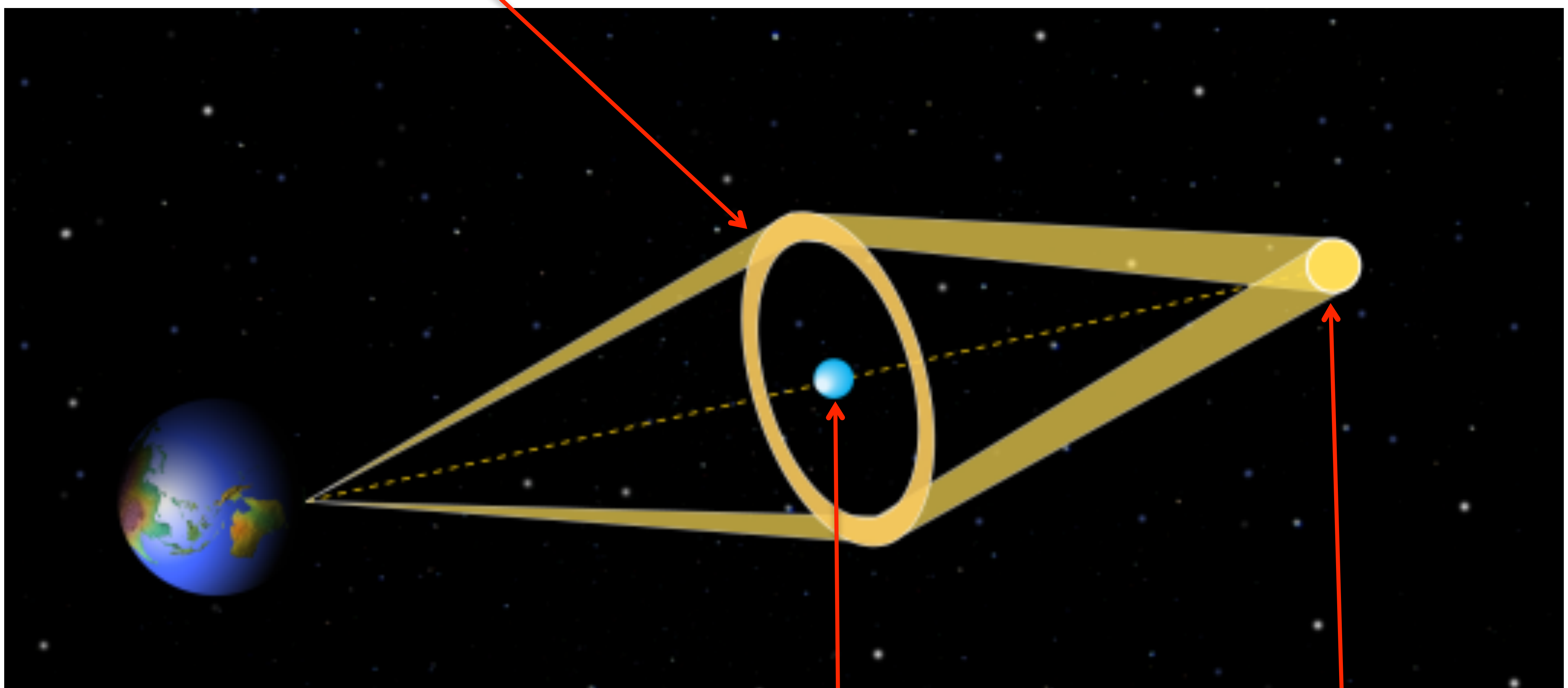

lens

source

If a lens is exactly (or very closely) aligned with a source there are magnified images of the source at (or near) an angle equal to the Einstein radius.

DISCUSSION

LENS-LIKE ACTION OF A STAR BY THE DEVIATION OF LIGHT IN THE GRAVITATIONAL FIELD

SOME time ago, R. W. Mandl paid me a visit and asked me to publish the results of a little calculation, which I had made at his request. This note complies with his wish.

The light coming from a star A traverses the gravitational field of another star B, whose radius is R_o. Let there be an observer at a distance D from B and at a distance x, small compared with D, from the extended central line $\overline{AB}$. According to the general theory of relativity, let α_o be the deviation of the light ray passing the star B at a distance R_o from its center.

For the sake of simplicity, let us assume that $\overline{AB}$ is large, compared with the distance D of the observer from the deviating star B. We also neglect the eclipse (geometrical obscuration) by the star B, which indeed is negligible in all practically important cases. To permit this, D has to be very large compared to the radius R_o of the deviating star.

It follows from the law of deviation that an observer situated exactly on the extension of the central line $\overline{AB}$ will perceive, instead of a point-like star A, a luminius circle of the angular radius β around the center of B, where

$$\beta = \sqrt{\alpha_o \frac{R_o}{D}}.$$

It should be noted that this angular diameter β does not decrease like $1/D$, but like $1/\sqrt{D}$, as the distance D increases.

Of course, there is no hope of observing this phenomenon directly. First, we shall scarcely ever approach closely enough to such a central line. Second, the angle β will defy the resolving power of our instruments. For, α_o being of the order of magnitude of one second of arc, the angle R_o/D, under which the deviating star B is seen, is much smaller. Therefore, the light coming from the luminous circle can not be distinguished by an observer as geometrically different from that coming from the star B, but simply will manifest itself as increased apparent brightness of B.

The same will happen, if the observer is situated at a small distance x from the extended central line $\overline{AB}$. But then the observer will see A as two point-like light-sources, which are deviated from the true geometrical position of A by the angle β, approximately.

The apparent brightness of A will be increased by the lens-like action of the gravitational field of B in the ratio q. This q will be considerably larger than unity only if x is so small that the observed positions of A and B coincide, within the resolving power of our instruments. Simple geometric considerations lead to the expression

$$q = \frac{l}{x} \cdot \frac{1 + \frac{x^2}{2l^2}}{\sqrt{1 + \frac{x^2}{4l^2}}},$$

where

$$l = \sqrt{\alpha_o D R_o}.$$

If we are interested mainly in the case $q \gg 1$, the formula

$$q = \frac{l}{x}$$

is a sufficient approximation, since $\frac{x^2}{l^2}$ may be neglected.

Even in the most favorable cases the length l is only a few light-seconds, and x must be small compared with this, if an appreciable increase of the apparent brightness of A is to be produced by the lens-like action of B.

Therefore, there is no great chance of observing this phenomenon, even if dazzling by the light of the much nearer star B is disregarded. This apparent amplification of q by the lens-like action of the star B is a most curious effect, not so much for its becoming infinite, with x vanishing, but since with increasing distance D of the observer not only does it not decrease, but even increases proportionally to $\sqrt{D}$.

ALBERT EINSTEIN

INSTITUTE FOR ADVANCED STUDY,
PRINCETON, N. J.

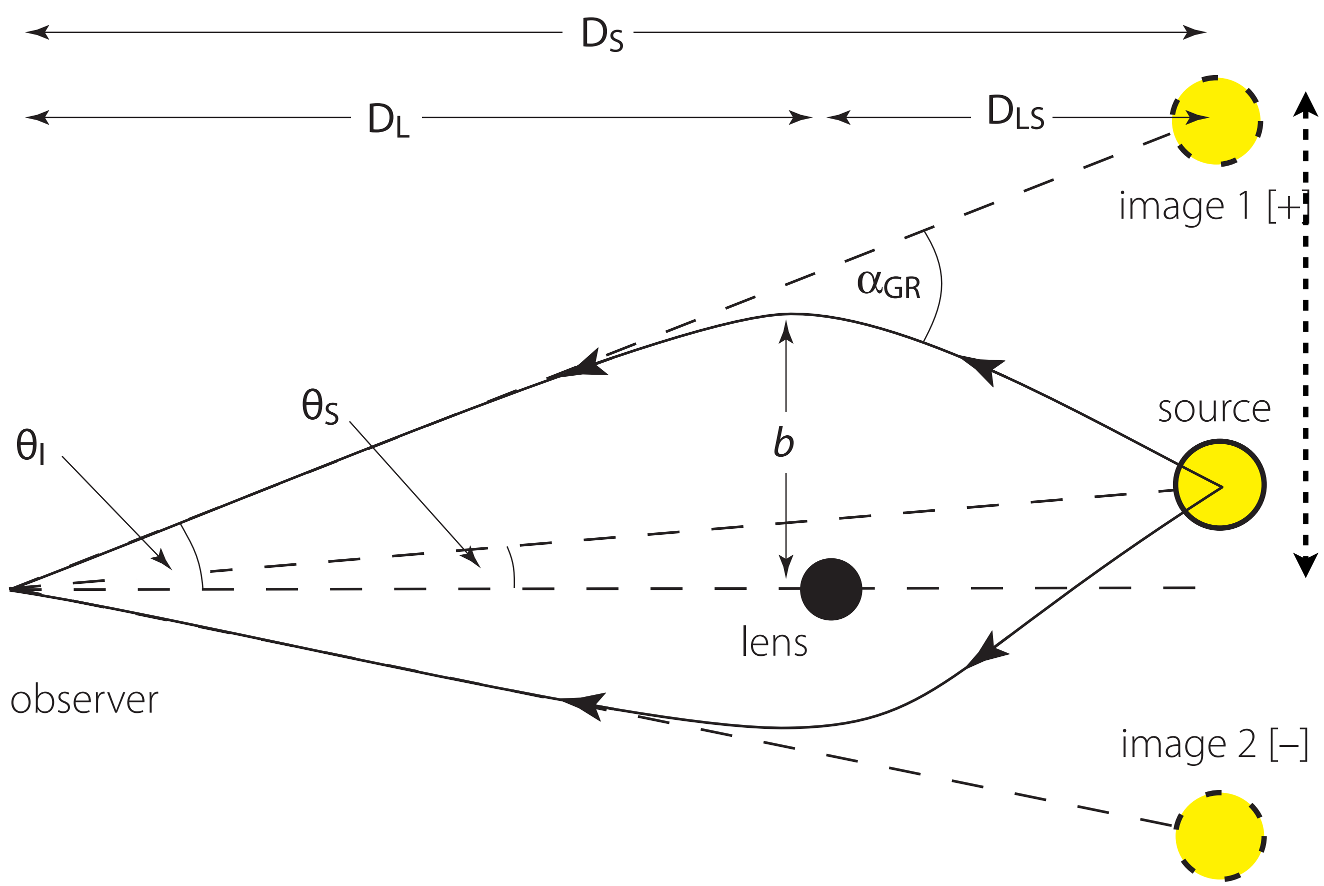

$$\alpha_{GR} = \frac{4GM_L}{c^2 b}$$

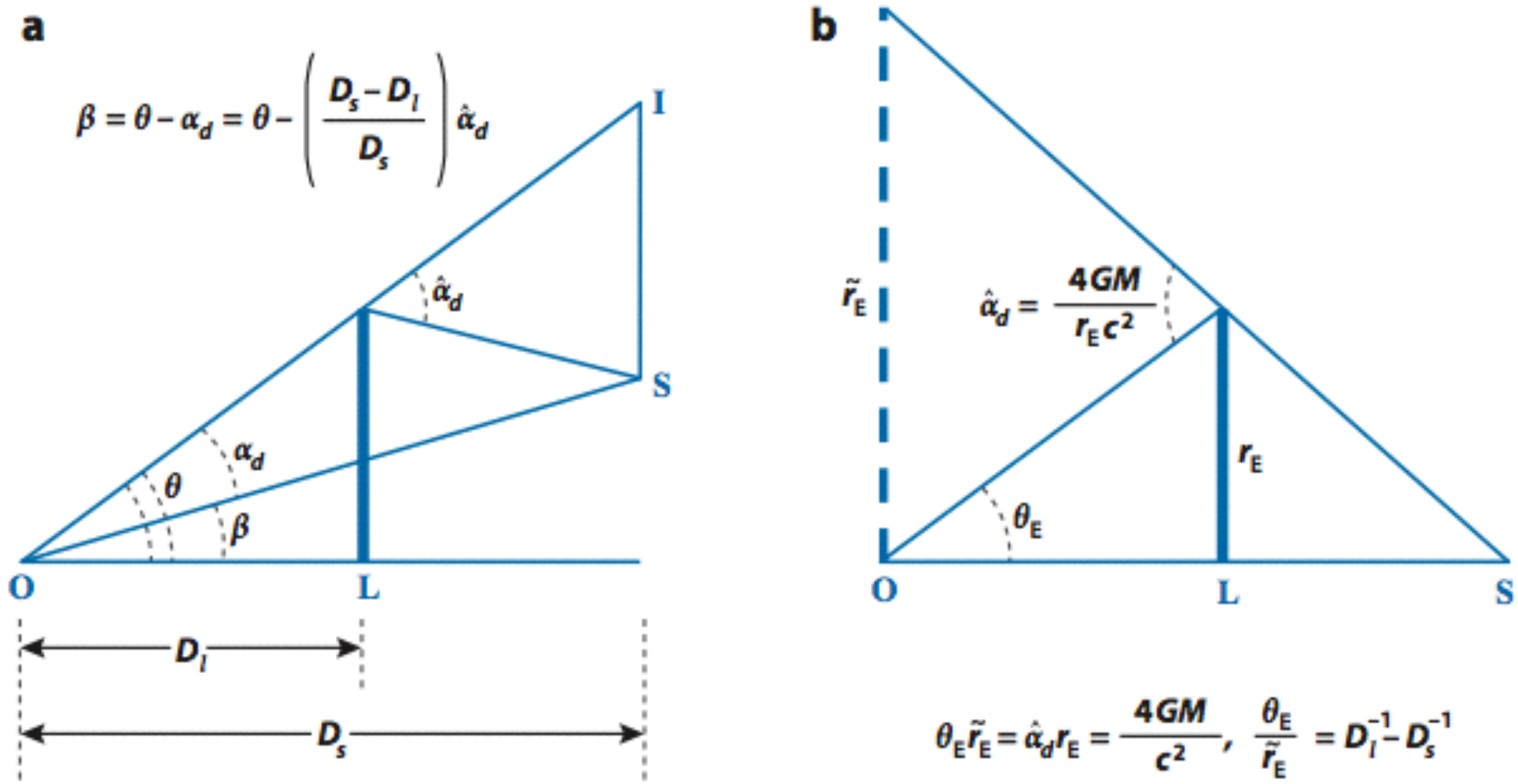

lens equation derived from geometry …
(what is the mapping between beta and theta?)

Gaudi (2012)

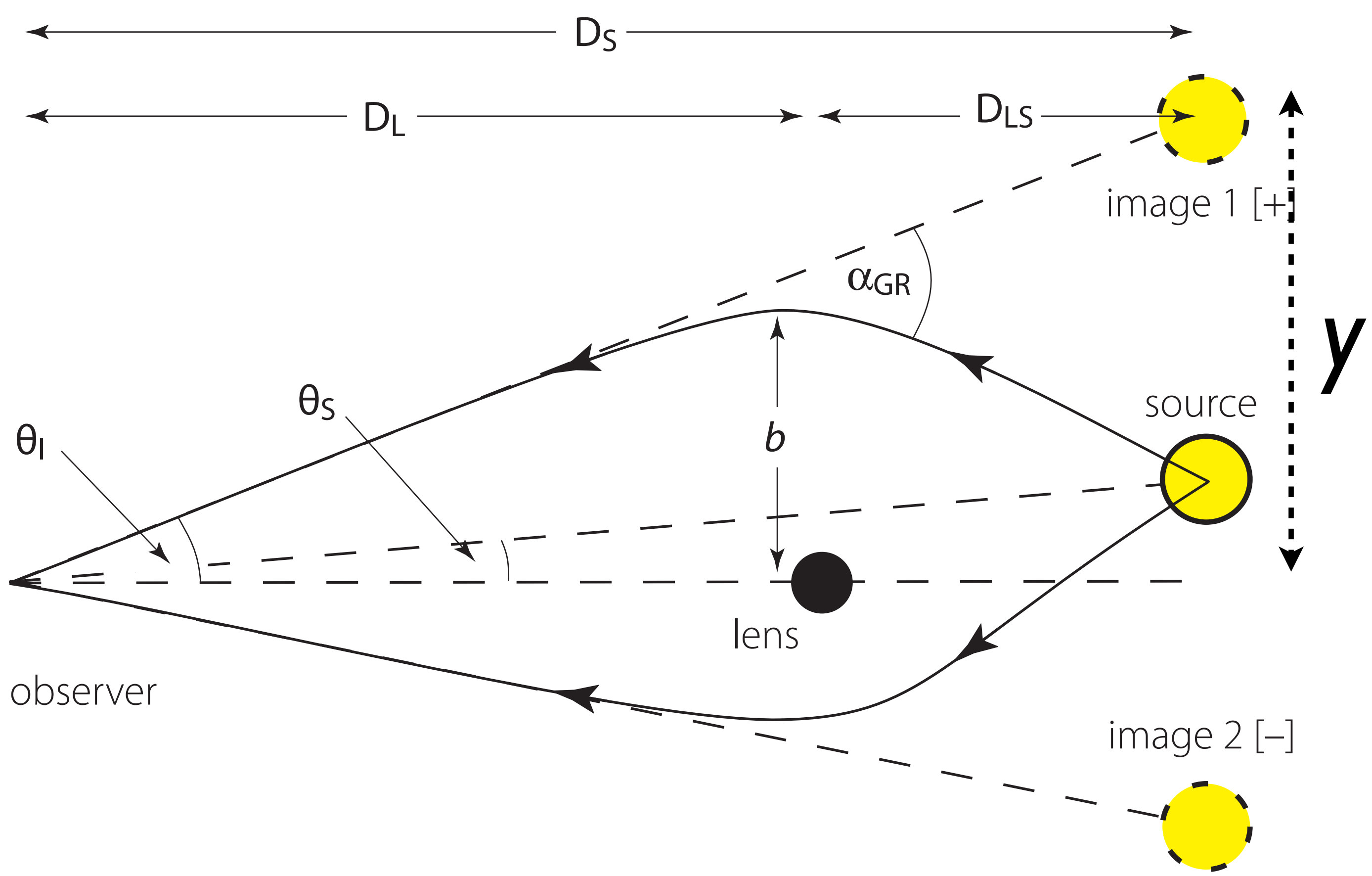

$$\alpha_{GR} = \frac{4GM_L}{c^2 b}$$

Recall that: $R_s = \dfrac{2GM_L}{c^2}$

$$\theta_s = \theta_1 - 2R_s \frac{D_{LS}}{D_L D_S} \frac{1}{\theta_1}$$

(the "lens equation")

$$u = y - y^{-1}$$

(basic quad. eq.)

$$y_\pm = \pm \frac{1}{2} \left(\sqrt{u^2 + 4} \pm u \right)$$

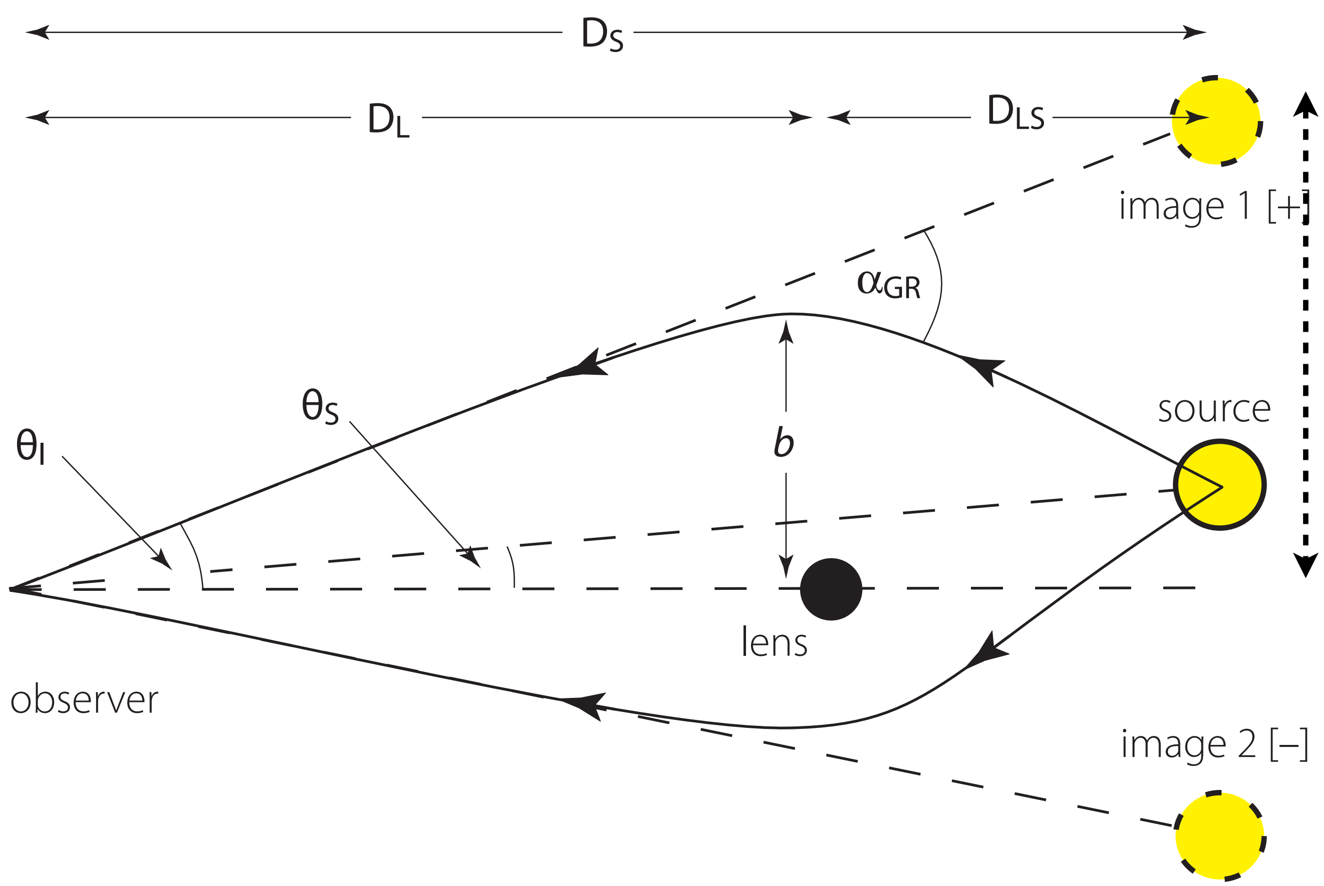

$$\alpha_{GR} = \frac{4GM_L}{c^2 b}$$

$$R_s = \frac{2GM_L}{c^2}$$

"angular and linear Einstein Radii"

$$\theta_E = \left[\alpha_{GR}\frac{D_{LS}}{D_L D_S}\right]^{1/2}$$

$$R_E = \theta_E D_L$$

$$\theta_s = \theta_1 - 2R_s \frac{D_{LS}}{D_L D_S}\frac{1}{\theta_1} \longrightarrow \theta_\pm = \frac{1}{2}\left(\theta_s \pm \sqrt{\theta_s^2 + 4\theta_E^2}\right)$$

(lens equation)

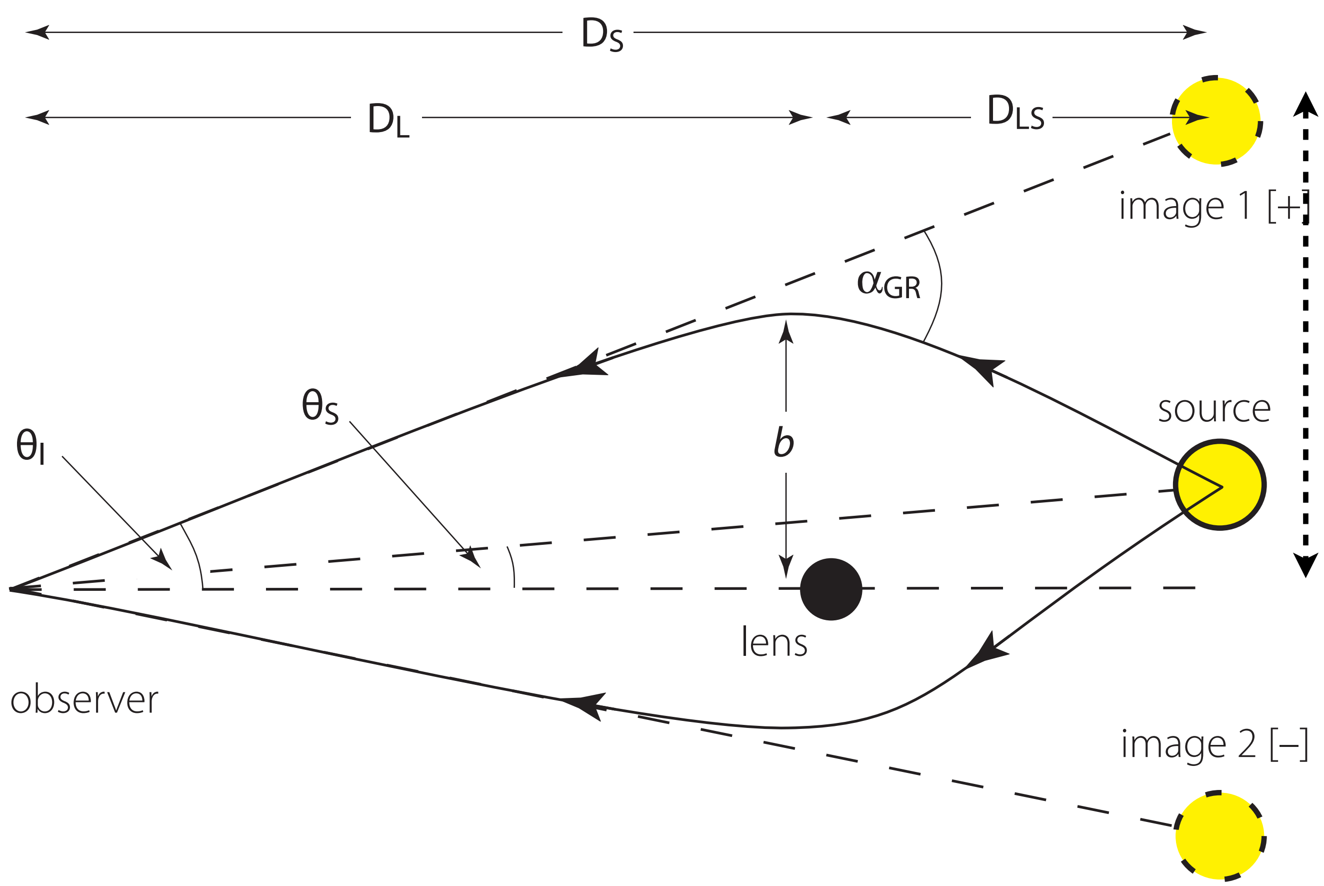

$$\alpha_{GR} = \frac{4GM_L}{c^2 b}$$

$$R_s = \frac{2GM_L}{c^2}$$

"angular and linear Einstein Radii"

$$\theta_E = \left[\alpha_{GR}\frac{D_{LS}}{D_L D_S}\right]^{1/2}$$

$$R_E = \theta_E D_L$$

For solar-mass lens
halfway to galactic center:

$$\theta_E \sim 1\ mas$$

$$R_E \sim 4\ AU$$

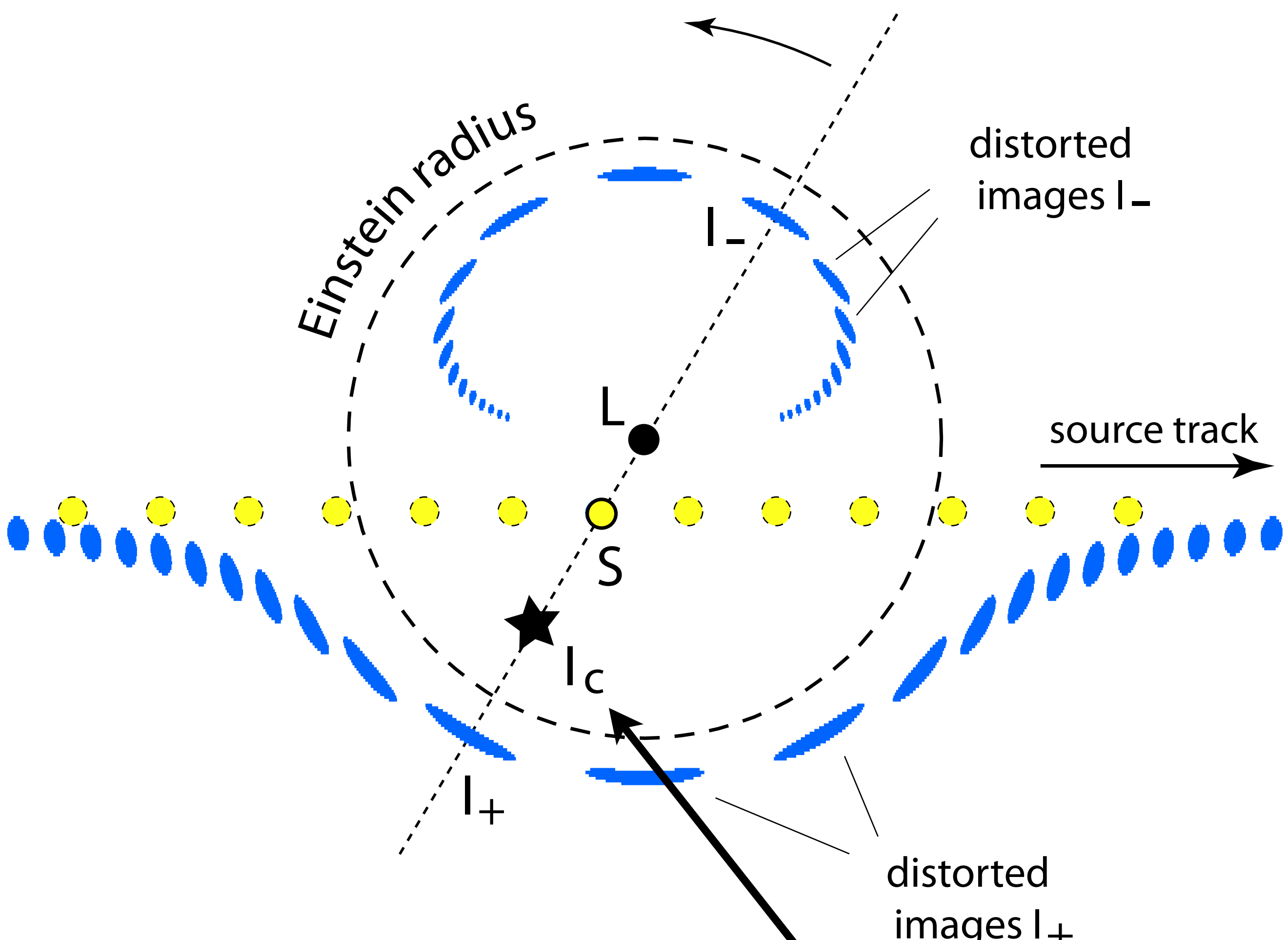

theta (~ mas) usually too small to resolve spatially, observe total flux

$$\theta_{\pm} = \frac{1}{2}\left(\theta_s \pm \sqrt{\theta_s^2 + 4\theta_E^2}\right)$$

for theta_s .ne. 0 —> two images!

image centroid moves in a non-linear path (think astrometry)

see also Paczynski (1996)

Microlensing (magnification)

Lensing conserves surface brightness, so think of lensing as a magnification of the surface. Flux = Area x surface brightness!

magnification is the ratio of image area to source area

Microlensing (magnification)

magnification is the ratio of image area to source area

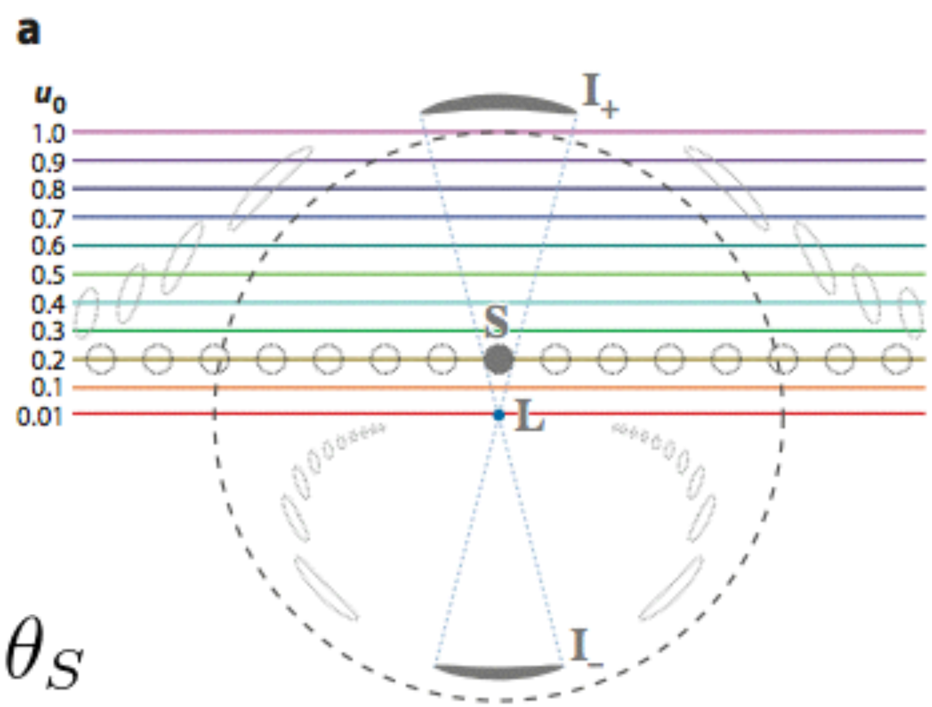

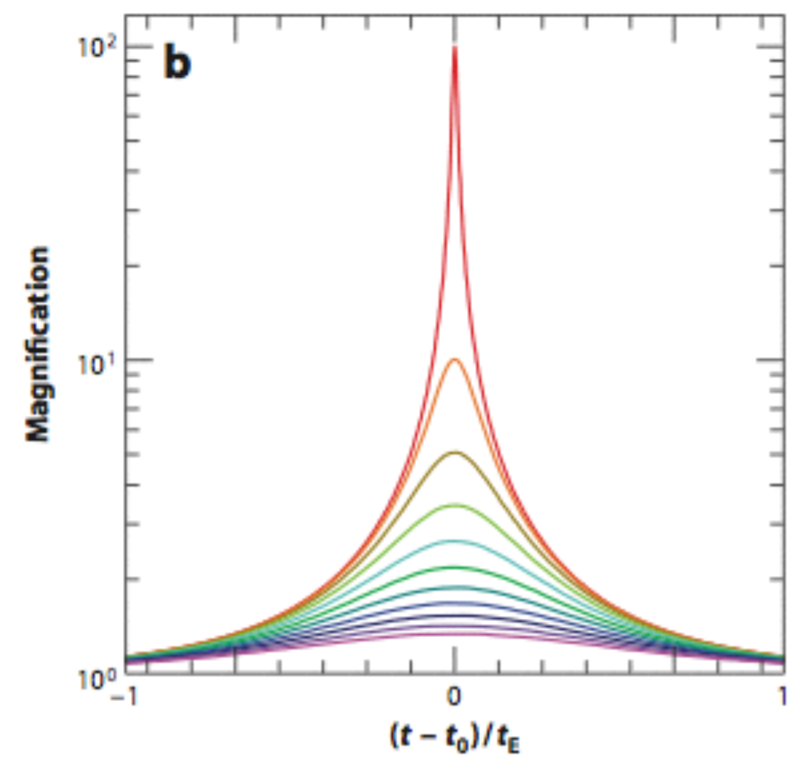

$$u = \frac{\theta_S}{\theta_E}$$

$$y = \frac{\theta}{\theta_E}$$

A ~ *l* x *w*

$$A_\pm = \left|\frac{y_\pm}{u}\frac{\mathrm{d}y_\pm}{\mathrm{d}u}\right| = \frac{1}{2}\left[\frac{u^2+2}{u\sqrt{u^2+4}} \pm 1\right]$$

(mag is time-dependent change in area)

(approximated by projected area above)

Gaudi (2012)

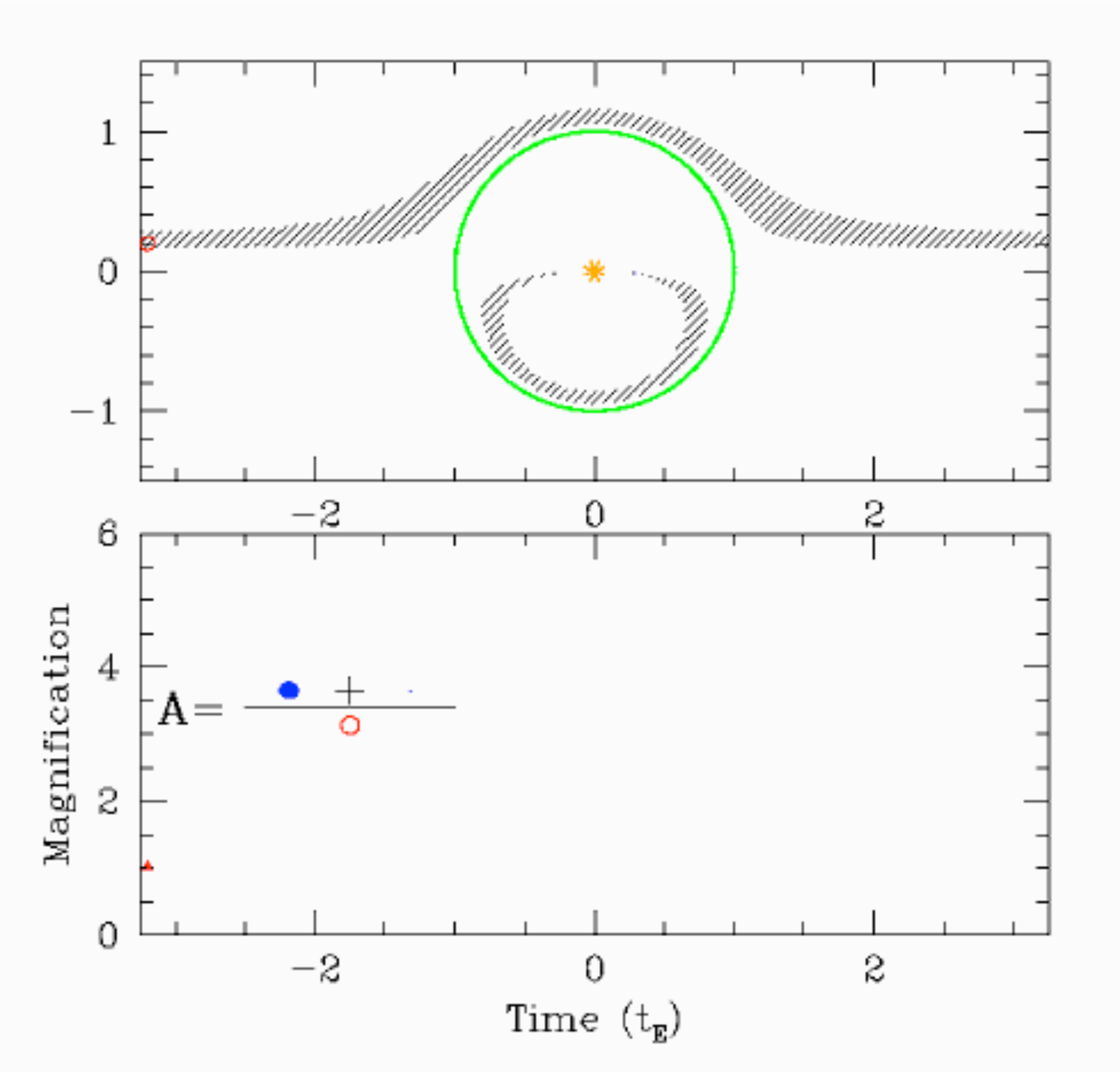

$$\theta_\pm = \frac{1}{2}\left(\theta_s \pm \sqrt{\theta_s^2 + 4\theta_E^2}\right)$$

$$A_\pm = \left|\frac{y_\pm}{u}\frac{\mathrm{d}y_\pm}{\mathrm{d}u}\right| = \frac{1}{2}\left[\frac{u^2+2}{u\sqrt{u^2+4}} \pm 1\right]$$ (time-dependent)

Animation is in the rest-frame of the lens (foreground star)

from Scott Gaudi: http://www.astronomy.ohio-state.edu/~gaudi/movies.html

single-lens observables

- time of peak-flux
- time of maximum magnification
- "duration", Einstein-radius crossing time, t_E

Events near the galactic bulge: t_E range ~ days to years

$$t_{\mathrm{E}} \simeq 24.8\,\mathrm{days}\left(\frac{M}{0.5\,\mathrm{M}_{\odot}}\right)^{1/2}\left(\frac{\pi_{\mathrm{rel}}}{125\,\mu\mathrm{as}}\right)^{1/2}\left(\frac{\mu_{\mathrm{rel}}}{10.5\,\mathrm{mas\ year}^{-1}}\right)^{-1}$$

depends on both lens mass and distance

Microlensing Probability (lensing optical depth)

P = Area covered by rings / Area of sky

$$\tau = \frac{1}{\Omega}\int_0^{D_s} n(D_l)\Omega D_l^2 \pi \theta_{\rm E}^2 dD_l = \int_0^{D_s} n(D_l) D_l^2 \pi \theta_{\rm E}^2 dD_l .$$

(For lensing < or = theta_E or A > ~ 1.34)

Microlensing Probability
(lensing optical depth)

P = Area covered by rings / Area of sky

$$\tau = \frac{1}{\Omega}\int_0^{D_s} n(D_l)\Omega D_l^2 \pi \theta_E^2 dD_l = \int_0^{D_s} n(D_l) D_l^2 \pi \theta_E^2 dD_l.$$

Microlensing Probability
(lensing optical depth)

P = Area covered by rings / Area of sky

$$\tau = \frac{1}{\Omega}\int_0^{D_s} n(D_l)\Omega D_l^2 \pi\theta_{\rm E}^2 dD_l = \int_0^{D_s} n(D_l) D_l^2 \pi\theta_{\rm E}^2 dD_l .$$

n-lens x area of one ring

$$n = \rho/M$$

$$\pi\theta_E^2 \propto M$$

$$\tau = \frac{4\pi G D_s^2}{c^2}\int_0^1 \rho(x)x(1-x)dx .$$

depends on *mass density* (not mass function) along line-of-sight.

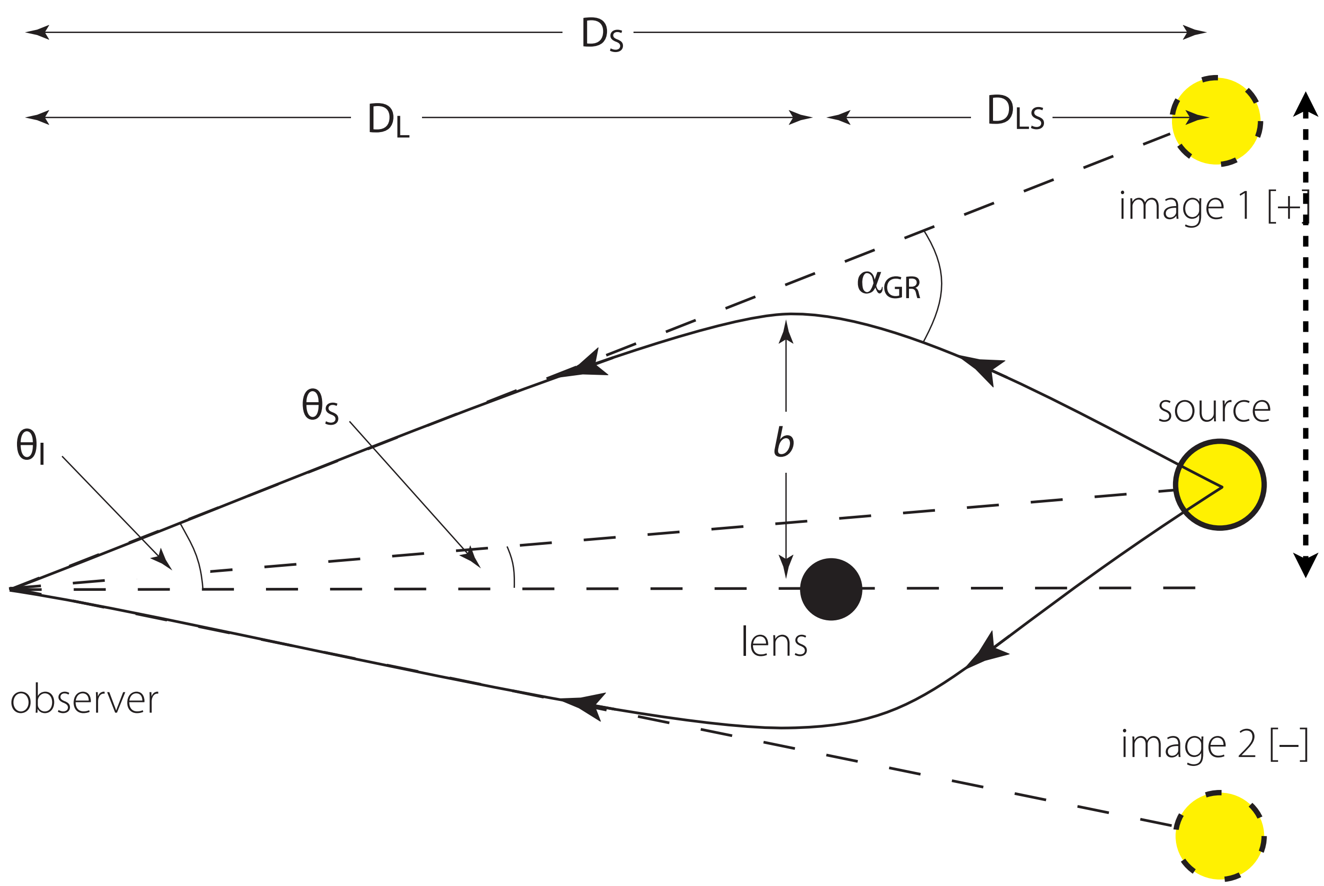

$$\alpha_{GR} = \frac{4GM_L}{c^2 b}$$

$$\boxed{\theta_E = \left[\alpha_{GR}\frac{D_{LS}}{D_L D_S}\right]^{1/2}}$$

$$R_E = \theta_E D_L$$

$$R_s = \frac{2GM_L}{c^2}$$

$$\theta_s = \theta_1 - 2R_s\frac{D_{LS}}{D_L D_S}\frac{1}{\theta_1} \longrightarrow \theta_\pm = \frac{1}{2}\left(\theta_s \pm \sqrt{\theta_s^2 + 4\theta_E^2}\right)$$

(lens equation)

Microlensing Event Rate

$$\Gamma = \frac{2}{\pi}\frac{\tau}{t_E} \qquad ; t_E = \frac{\theta_E}{\mu_{rel}}$$

does depend on mass function
along line-of-sight

look to the Bulge!

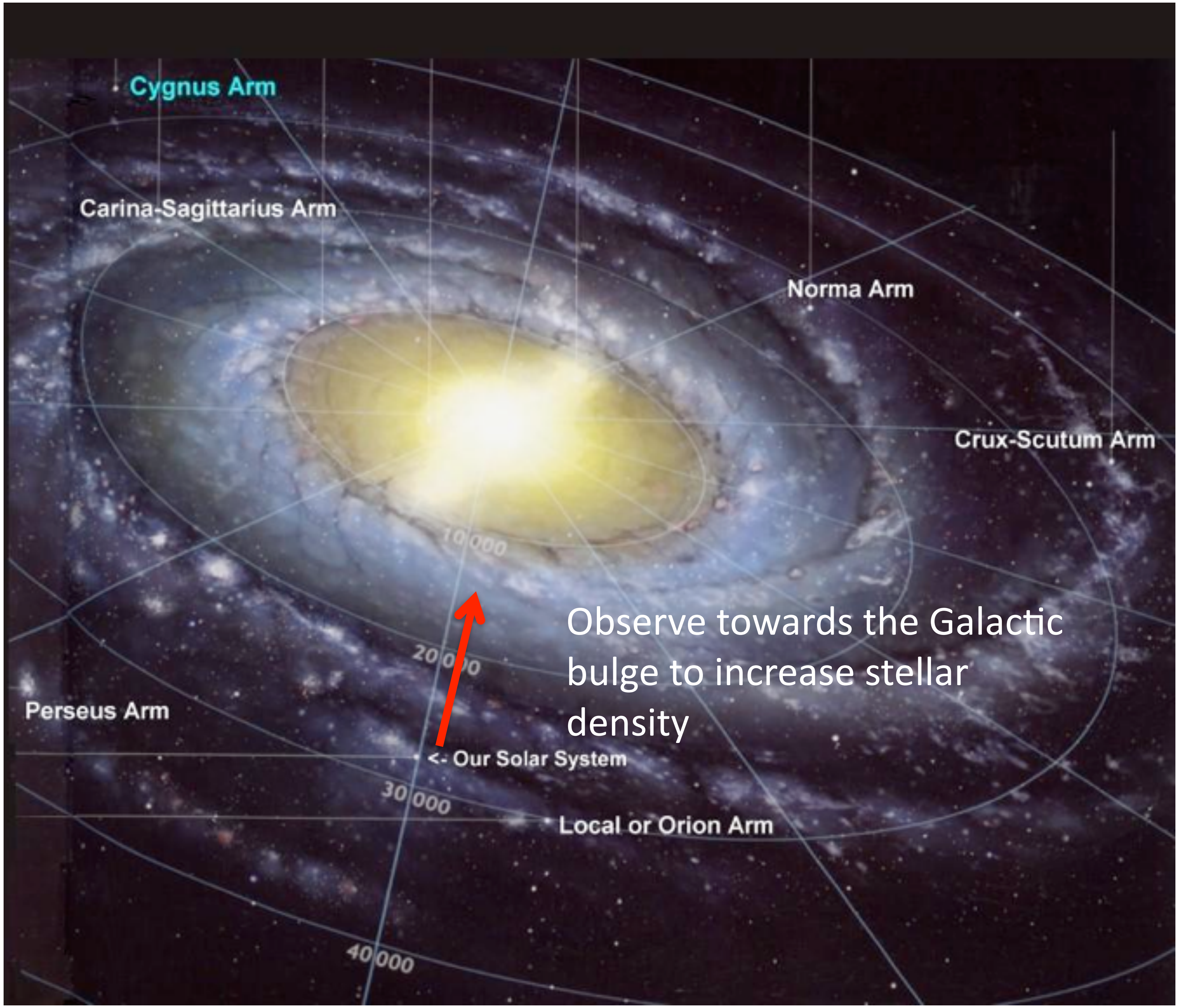

microlensing is rare ...

- lensing optical depth toward Galactic Bulge is ~ 10^{-6}
- median timescale of event ~ 20 days
- rate for lens event / star ~ 10^{-5} per year!
- OGLE survey monitors ~ 2.5×10^{8} sources over 80 square degrees ~ 1,500 events / 8 month observing window.

Microlensing + planets

Binary Lens: adds three more parameters:

- mass ratio
- projected separation of binary at time of event
- angle between source-lens trajectory and binary axis at time of event

Lens Source

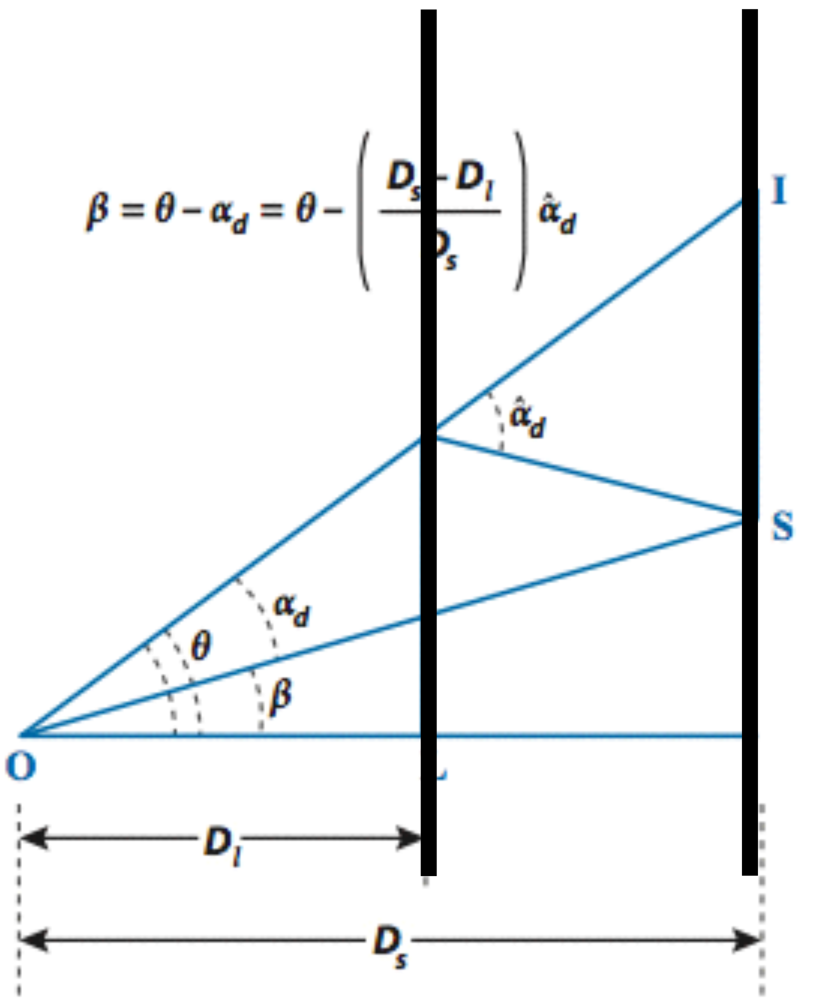

mapping between
source and lens planes
(beta <----> theta)

solution to lens magnification for multiple lens:

$$A_j = \frac{1}{\det J}\bigg|_{\theta=\theta_j}$$

caustic curves: *source* positions where det J = 0

critical curves: *image* positions

Gaudi (2012)

pretty “caustics”

pretty “caustics”

Caustics from http://www.mpa-garching.mpg.de/mpa/

“caustics” (typically 2 to 3 for one planet)

q = 0.003

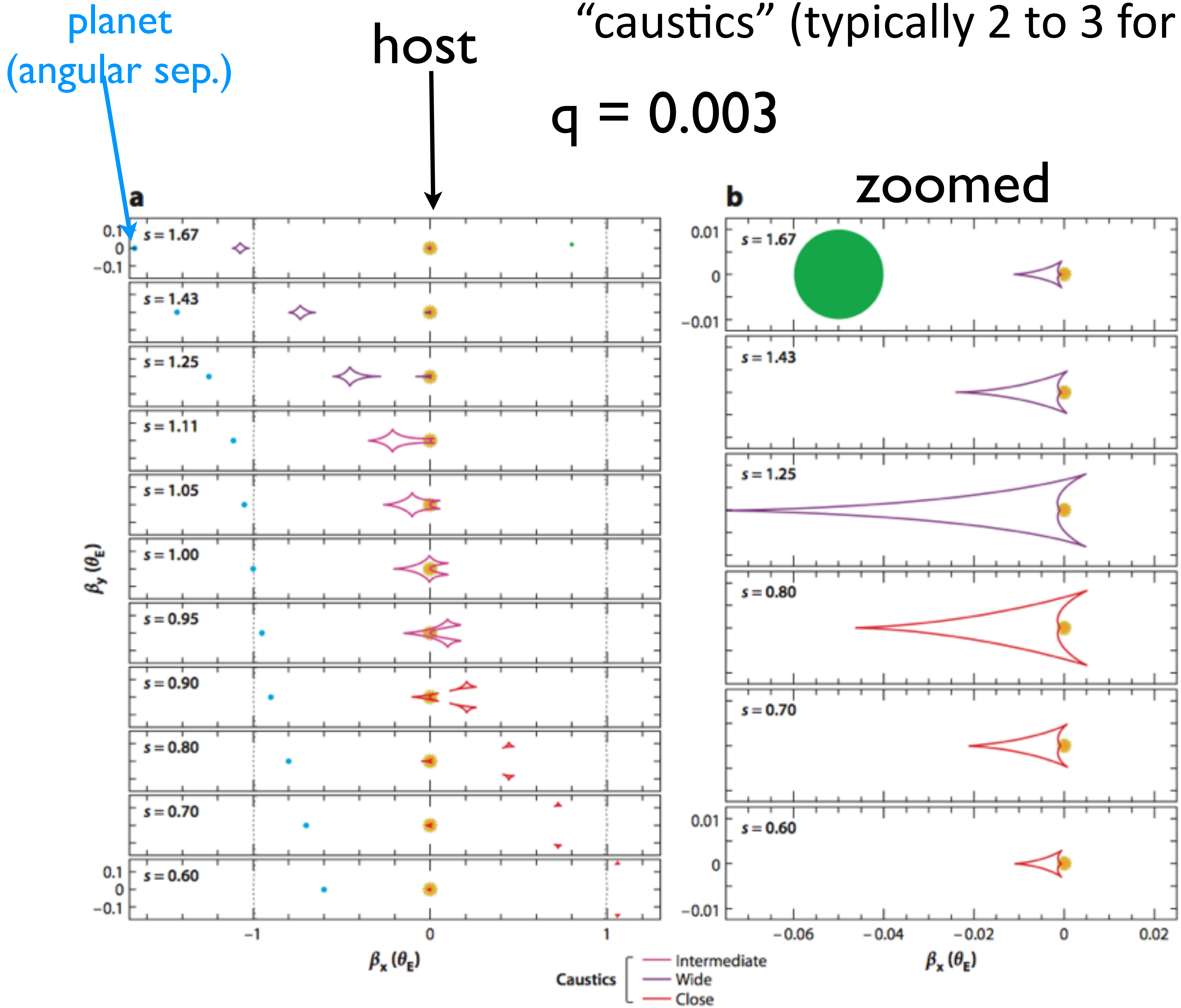

Microlensing

Planetary perturbation example:

Magnified images along the Einstein ring pass near the planet and are magnified again (“the source crosses the planetary caustic”)

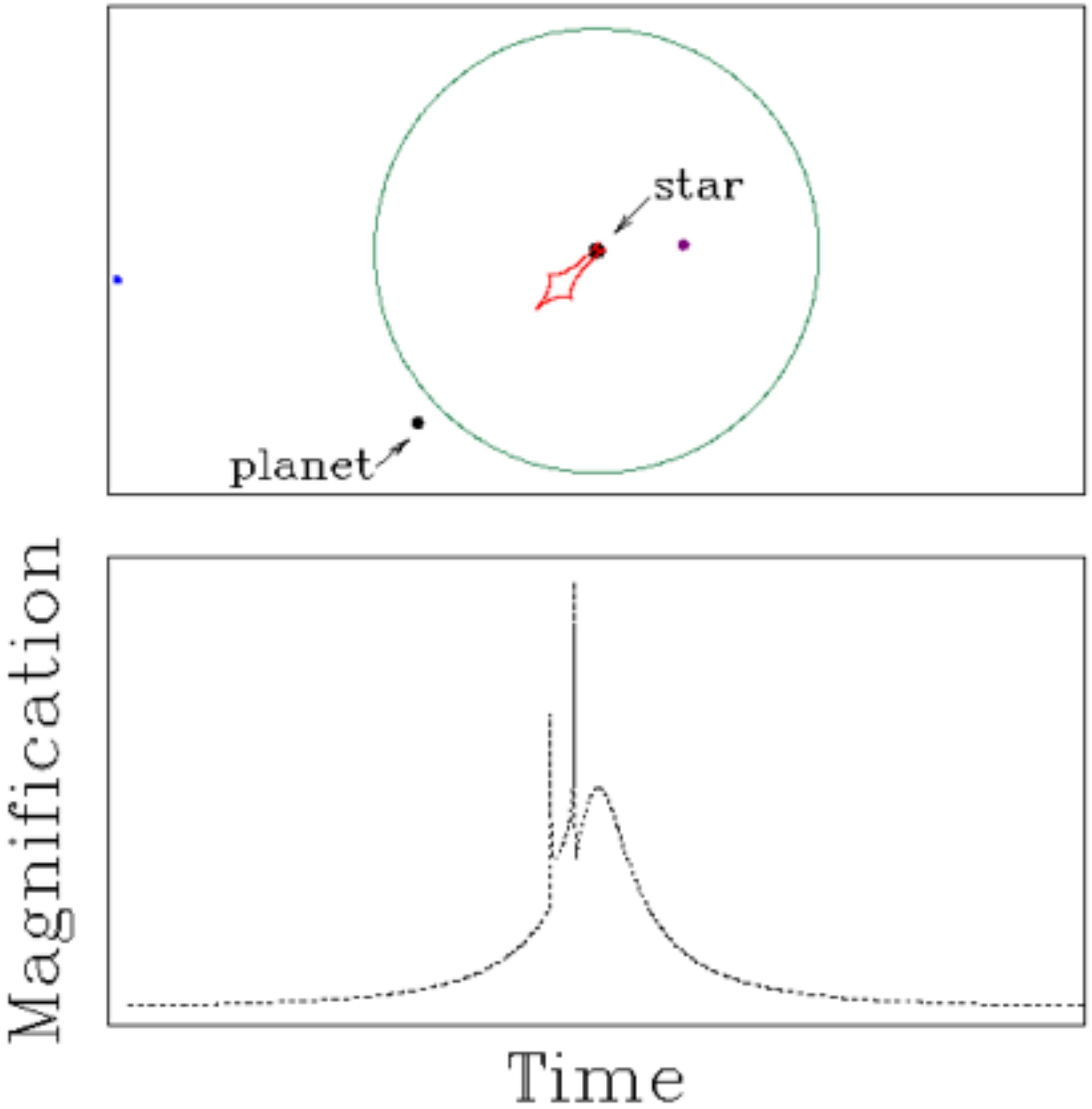

planet outside and near ring:

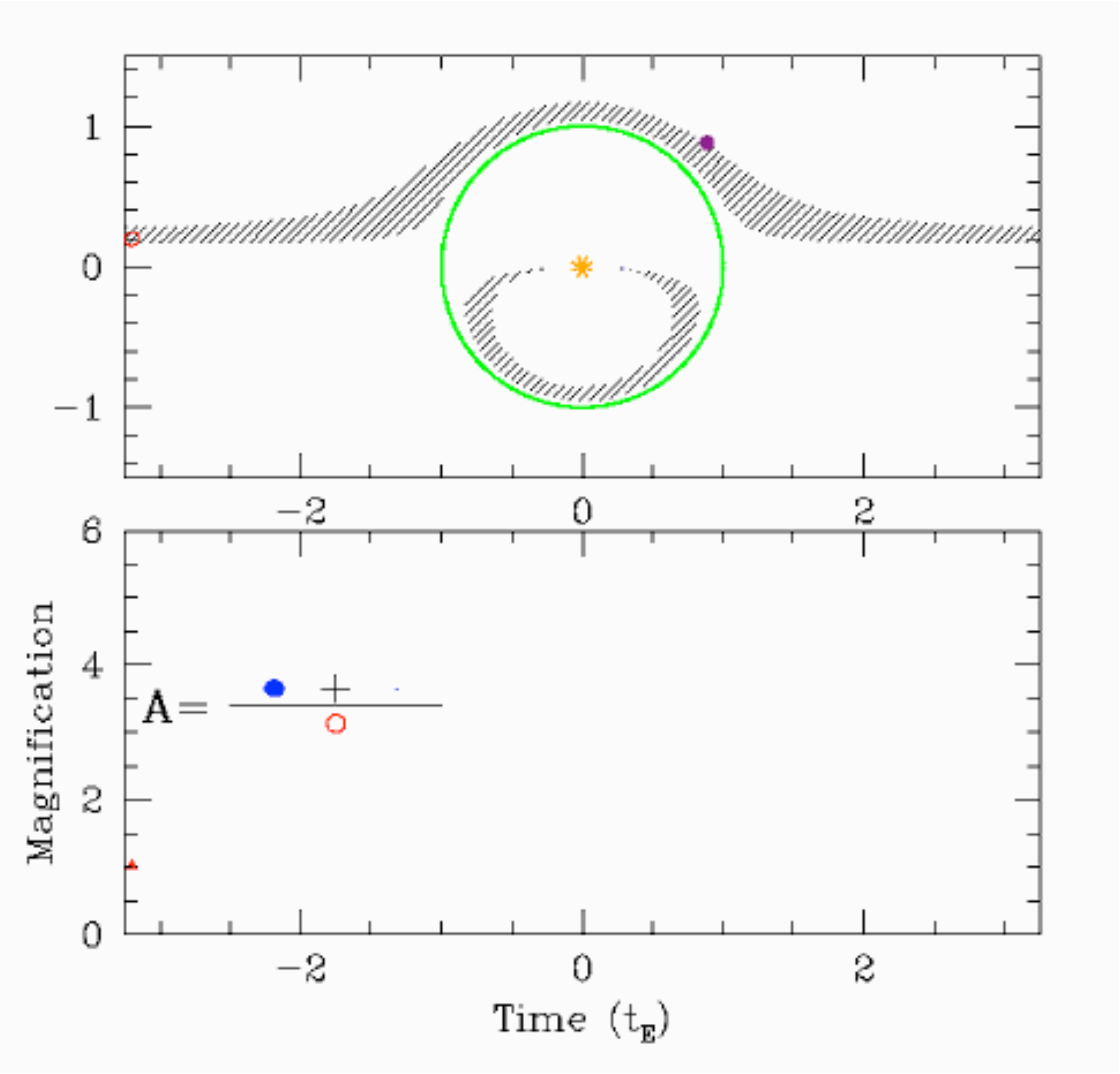

For solar-mass lens halfway to galactic center:

$$\theta_E \sim 1\ mas$$

$$R_E \sim 4\ AU$$

effect of changing planet/source track angle:

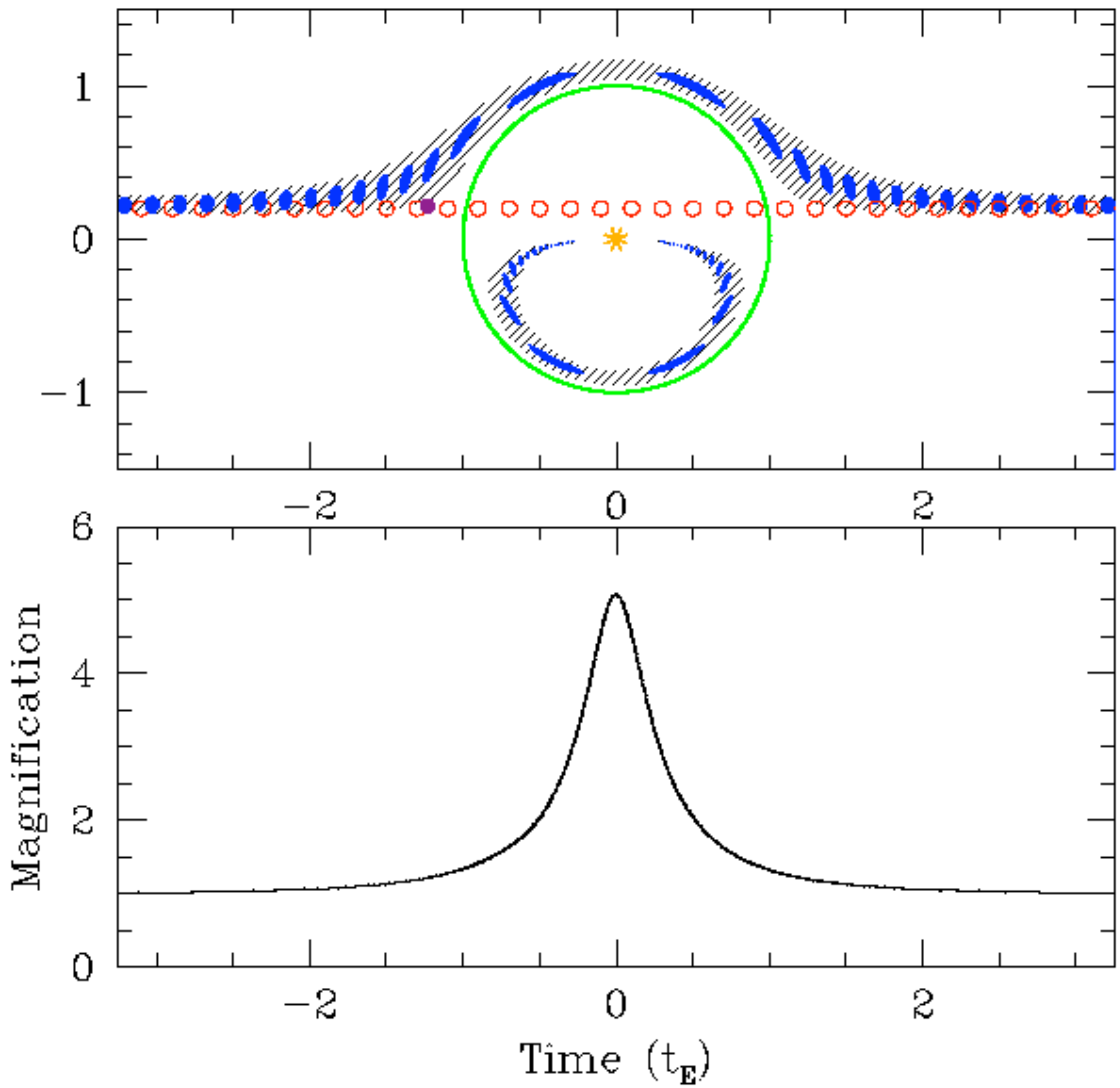

effect of changing separation:

http://www.astronomy.ohio-state.edu/~gaudi/Movies/lcp_b.gif

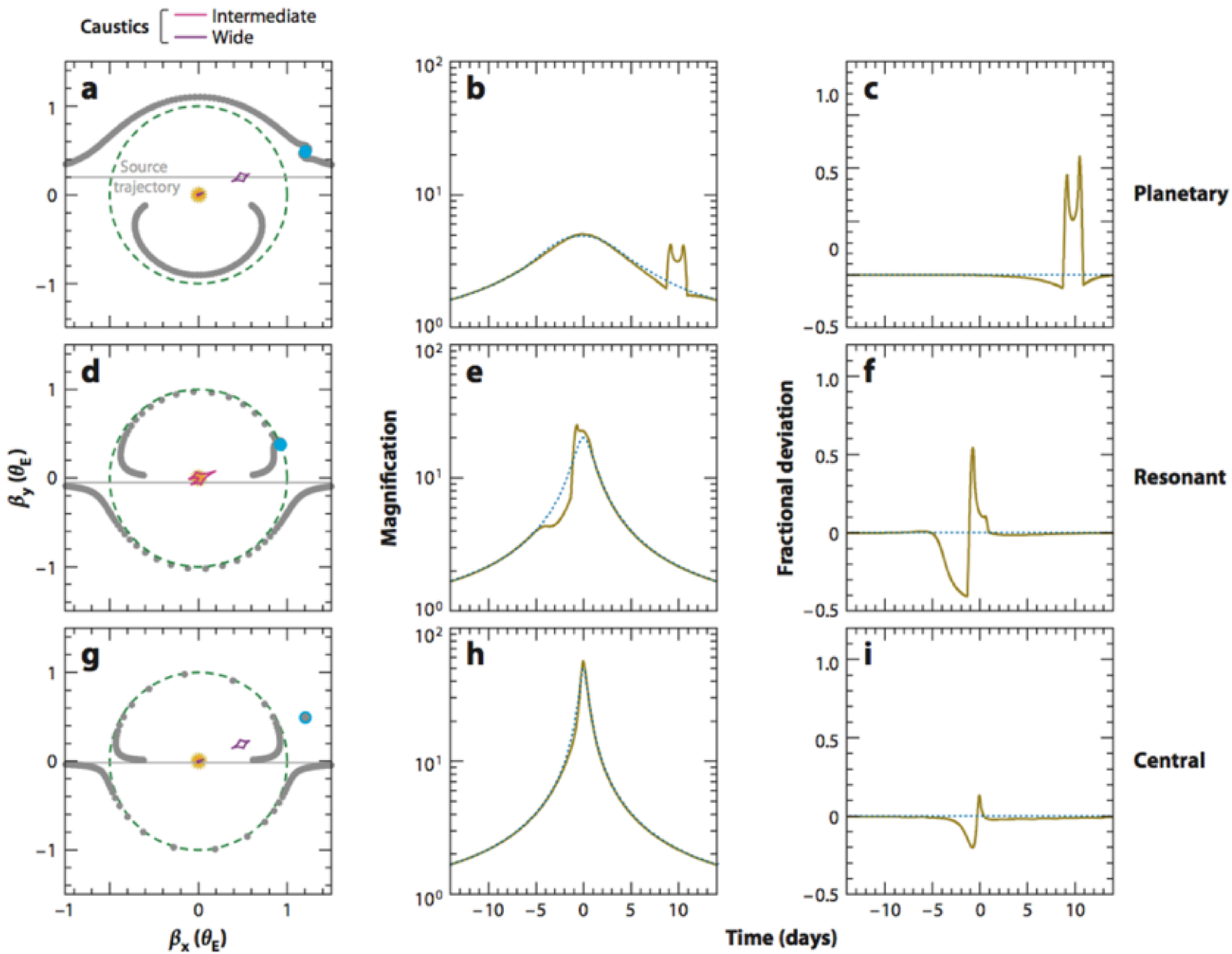
Caustics
Intermediate
Wide
a
b
c
d
e
f
g
h
i
Source trajectory
Planetary
Resonant
Central
Magnification
Fractional deviation
β_y (θ_E)
β_x (θ_E)
Time (days)

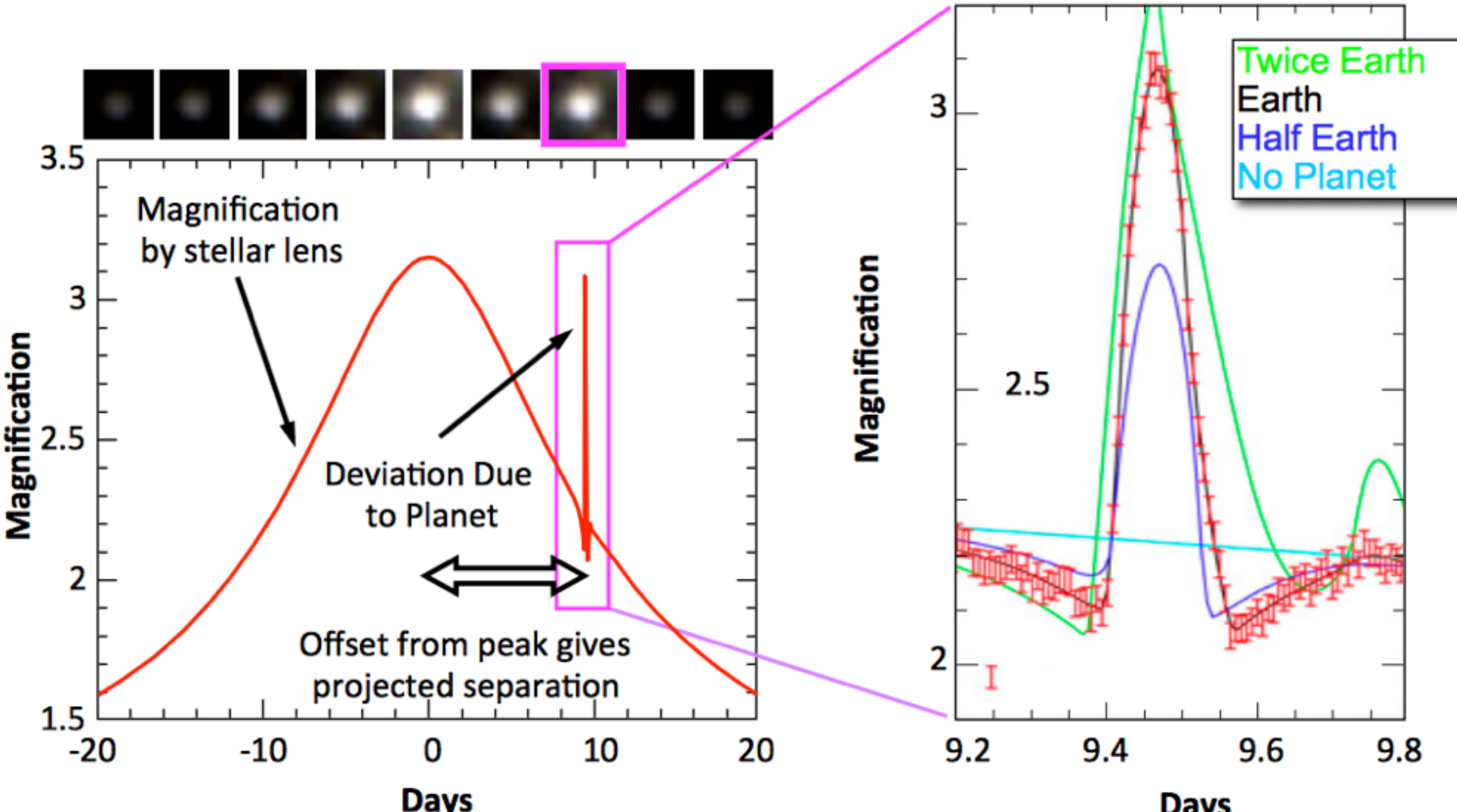

Bennett + NASA

What can you learn?

Planetary Perturbation

- Same as for the main event: measure time of maximum magnification, maximum magnification, and duration

- The duration is proportional to $q^{1/2}t_E$. With t_E from the main event, you get $q = M_p/M_s$

- The time and magnitude of the perturbation give the separation and position angle of the planet

What can you learn?

Planet-Star System

- With the mass ratio (q), you need to find some way to get the lens mass
- Finite source effects, and some assumptions about the source distance, give you a mass-distance relation for the lens
- Measure photometry and/or spectroscopy of the lens itself
- Measure the proper motion of the system
- Detect the microlens parallax
- Detect orbital motion of the planets

Powerful statistical probe of exoplanet population:

- very sensitive to planets > snow line
- magnification does not depend on planet mass (sensitive to low mass planets)
- sensitive to long-period planets (and free-floaters)
- probes galactic planet distribution
- detects multi-planet systems.

Microlensing Highlights: OGLE-2005-BLG-390Lb

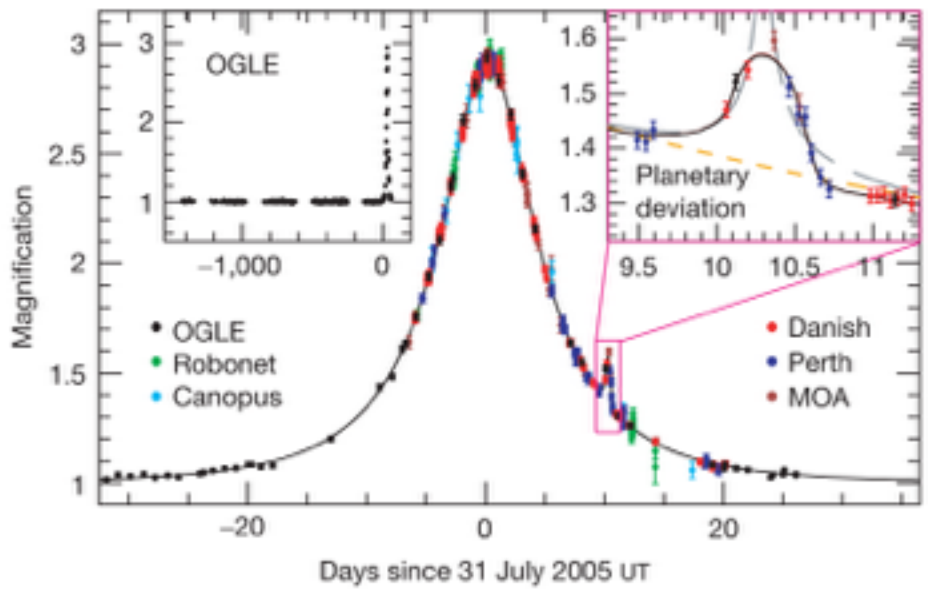

Figure 1 | The observed light curve of the OGLE-2005-BLG-390 microlensing event and best-fit model plotted as a function of time. Error bars are 1σ. The data set consists of 650 data points from PLANET Danish (ESO La Silla, red points), PLANET Perth (blue), PLANET Canopus (Hobart, cyan), RoboNet Faulkes North (Hawaii, green), OGLE (Las Campanas, black), MOA (Mt John Observatory, brown). This photometric monitoring was done in the I band (with the exception of the Faulkes R-band data and the MOA custom red passband) and real-time data reduction was performed with the different OGLE, PLANET and MOA data reduction pipelines. Danish and Perth data were finally reduced by the image subtraction technique[19] with the OGLE pipeline. The top left inset shows the OGLE light curve extending over the previous 4 years, whereas the top right one shows a zoom of the planetary deviation, covering a time interval of 1.5 days. The solid curve is the best binary lens model described in the text with $q = 7.6 \pm 0.7 \times 10^{-5}$, and a projected separation of $d = 1.610 \pm 0.008 R_E$. The dashed grey curve is the best binary source model that is rejected by the data, and the dashed orange line is the best single lens model.

Beaulieu et al. 2006, Nature, 439, 437

$M_p = 5.5\ M_{earth}$
$a = 2.6$ AU
$M_s = 0.20\ M_{sun}$
(with big errors)

=> Super-Earths must be common

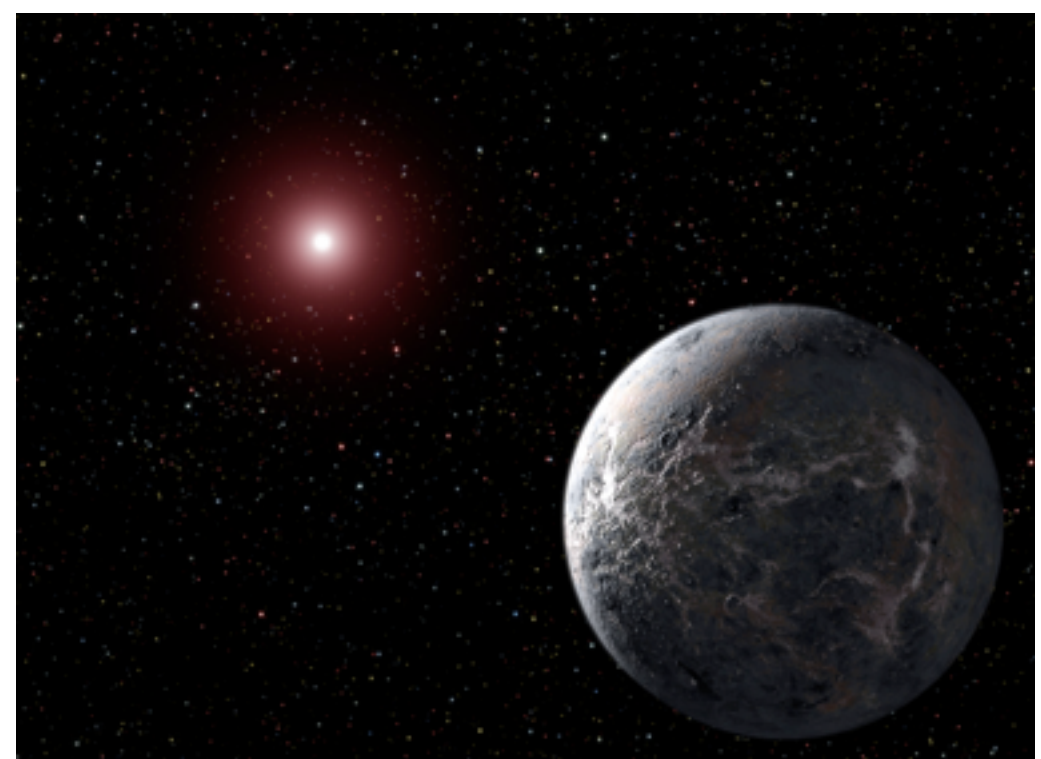

Microlensing Highlights: OGLE-2006-BLG-109Lb

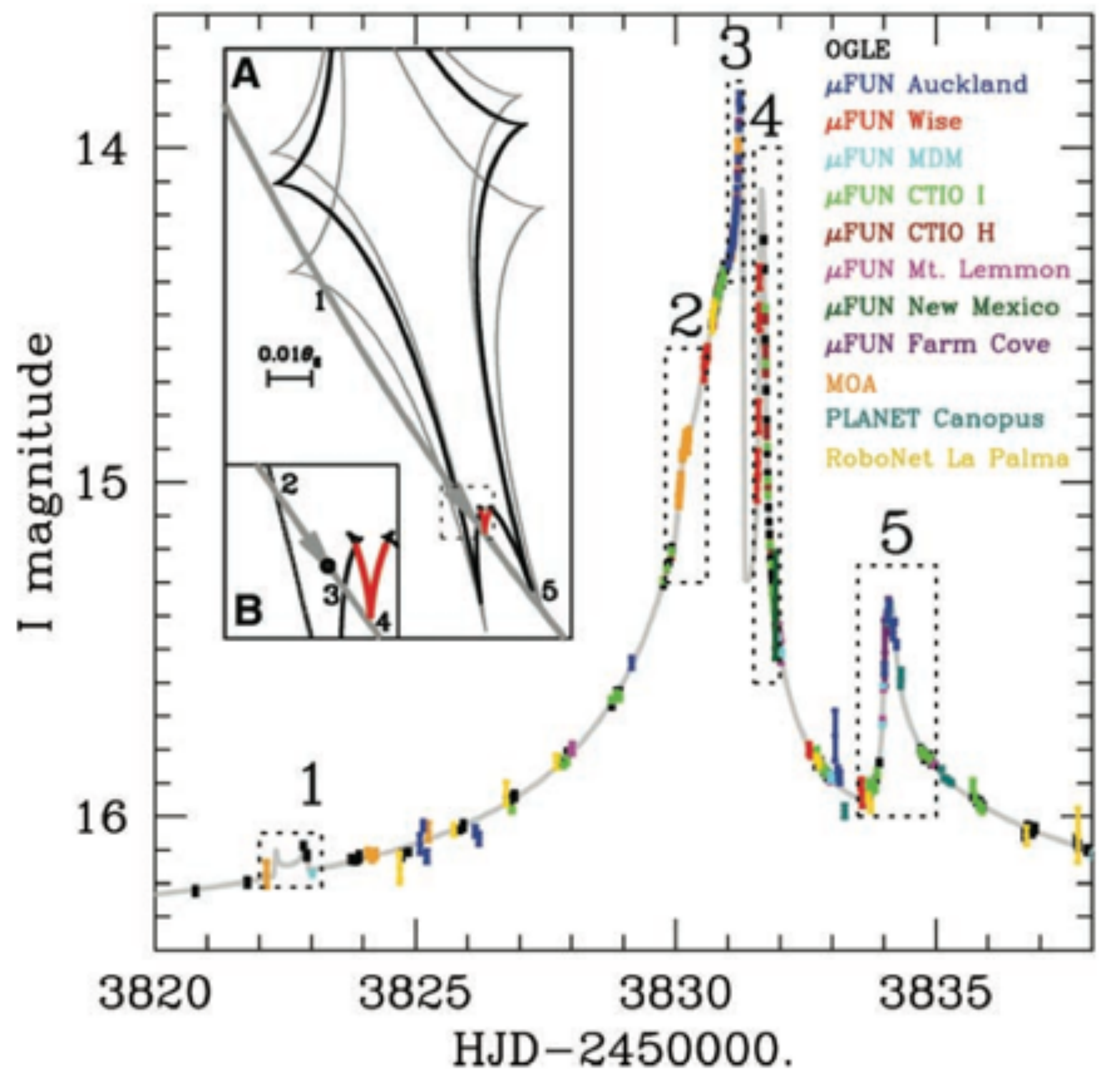

Fig. 1. Data and best-fit model of the OGLE-2006-BLG-109Lb,c two-planet system. The data have been binned for clarity, although the fitting procedures used the unbinned data. Data from each different observatory/filter combination (as indicated by the color scheme) have been aligned using a linear fit to the magnification, which introduces negligible uncertainties. Only data near the peak of the event are shown (the unlensed magnitude is $I = 16.42$). **(A)** The source trajectory through the caustic created by the two-planet system is shown as the dark gray curve with the arrow indicating the direction of motion. The horizontal line shows an angular scale of 0.01 θ_E, or ~15 μas. The shape and orientation of the caustic due to both planets at the peak of the event is shown by the black curve. The five light-curve features detailed in Fig. 2 are caused by the source crossing or approaching the caustic; the approximate locations of the features are labeled with numbers. The majority of the caustic (in black) is due to only the outer (Saturn-analog) planet; this portion of the caustic explains four of the five features. The portion arising from the second (Jupiter-analog) planet is highlighted in red. This additional cusp in the caustic is required to explain the fourth feature in the light curve; as such, the fourth feature signals the presence of a second (Jupiter-analog) planet. Because of the orbital motion of the Saturn-analog planet, the shape and orientation of the caustic changes over the course of the event. The light gray curves show the caustic at the time of features 1 and 5. **(B)** A zoom of the source trajectory and caustic near the times of the second, third, and fourth features. The circle shows the size of the source.

A Jupiter-Saturn analog system around a $M = 0.5\ M_{sun}$ star

Orbital motion of the outer planet was detected

Gaudi et al. 2008, Science, 319, 927

Microlensing Highlights: Unbound Planets?

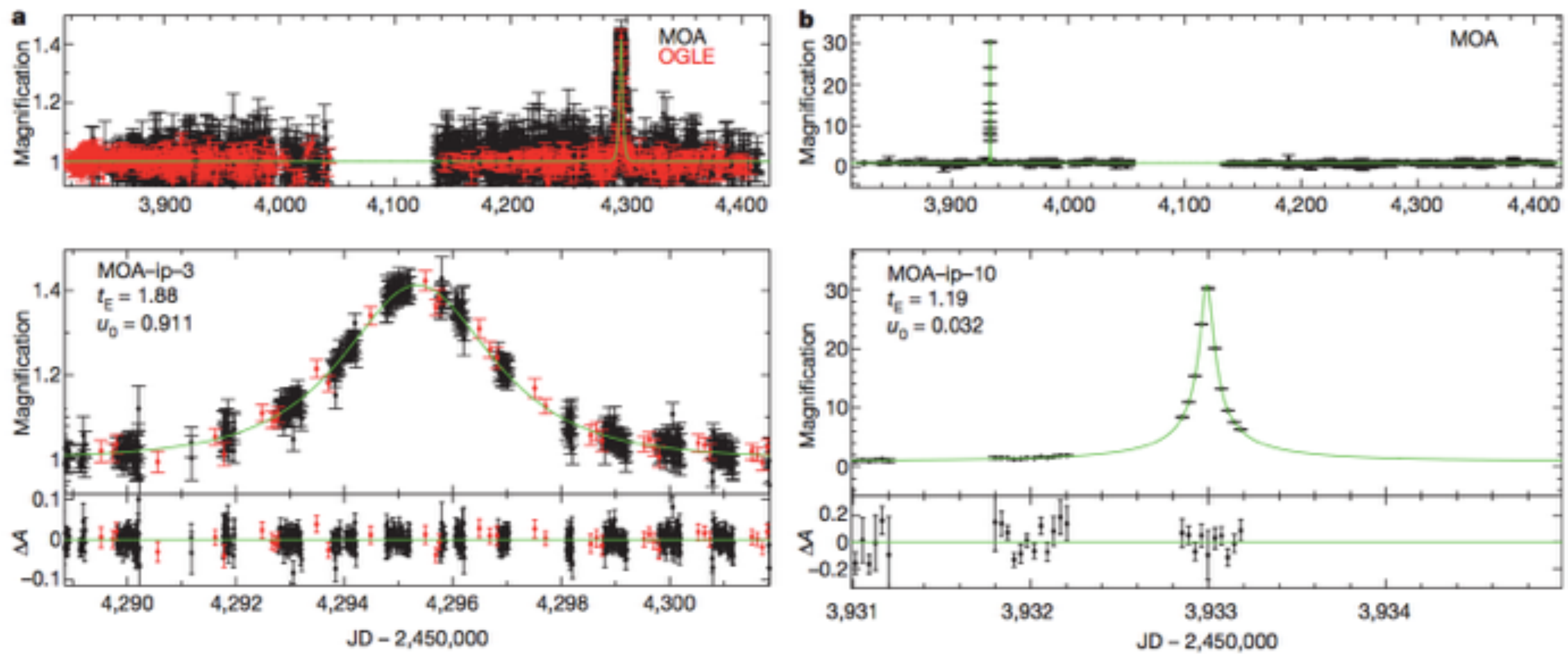

Figure 1 | Light curves of event MOA-ip-3 and event MOA-ip-10. These have the highest signal-to-noise ratio of the ten microlensing events with $t_E < 2$ days (see Supplementary Fig. 1 for the others). MOA data are in black and OGLE data are in red, with error bars indicating the s.e.m. **a**, MOA-ip-3 light curve; **b**, MOA-ip-10 light curve. The green lines represent the best-fit microlensing model light curves. For each event, the upper panel shows the full two-year light curve, the middle panel is a close-up of the light-curve peak, and the bottom panel shows the residuals from the best-fit model in units of the magnification, ΔA. u_0 indicates the source–lens impact parameter in units of the Einstein radius. The second phase of MOA, MOA-II, carried out a very-high-cadence photometric survey of 50 million stars in 22 bulge fields (of 2.2 deg^2 each) with a 1.8-m telescope at Mt John Observatory in New Zealand. MOA detects 500–600 microlensing events during eight months observation every year. In 2006–2007, MOA observed two central bulge fields every 10 min, and other bulge fields with a 50 min cadence, which resulted in about 8,250 and 1,660–2,980 images, respectively. This strategy enabled MOA to detect very short events with $t_E < 2$ days. Since 2002, the OGLE-III survey has monitored the bulge with the 1.3-m Warsaw telescope at Las Campanas Observatory, Chile, with a smaller field-of-view but better astronomical seeing than MOA. The OGLE-III observing cadence was 1–2 observations per night, but the OGLE photometry is usually more precise and fills gaps in the MOA light curves owing to the difference in longitude.

Sumi et al. 2011, Nature, 473, 349

$1.8^{+1.7}_{-0.8}$ planetary mass objects at >10 AU per star

TRIPLE MICROLENS OGLE-2008-BLG-092L: BINARY STELLAR SYSTEM WITH A CIRCUMPRIMARY URANUS-TYPE PLANET

Poleski et al. (2014)

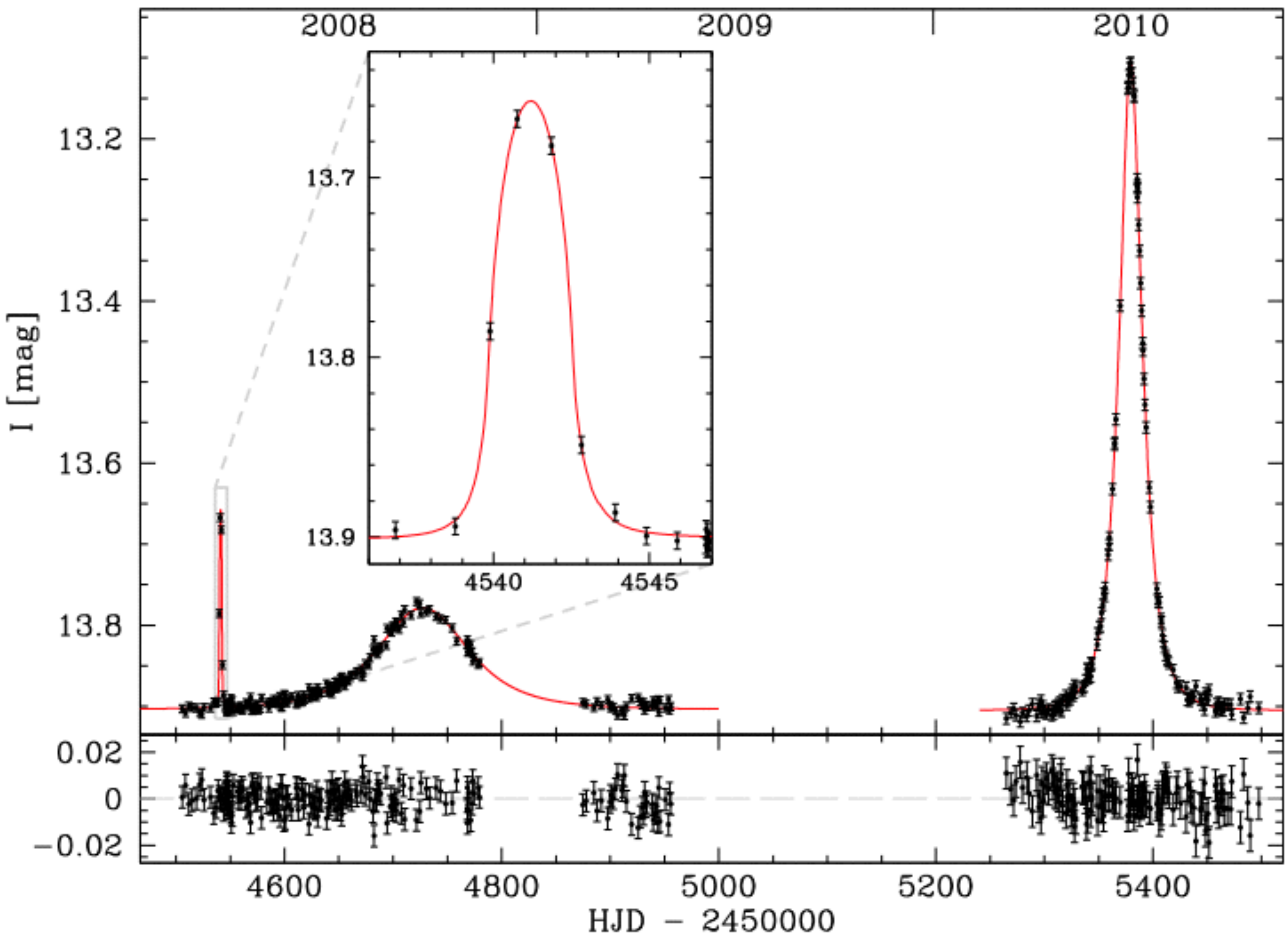

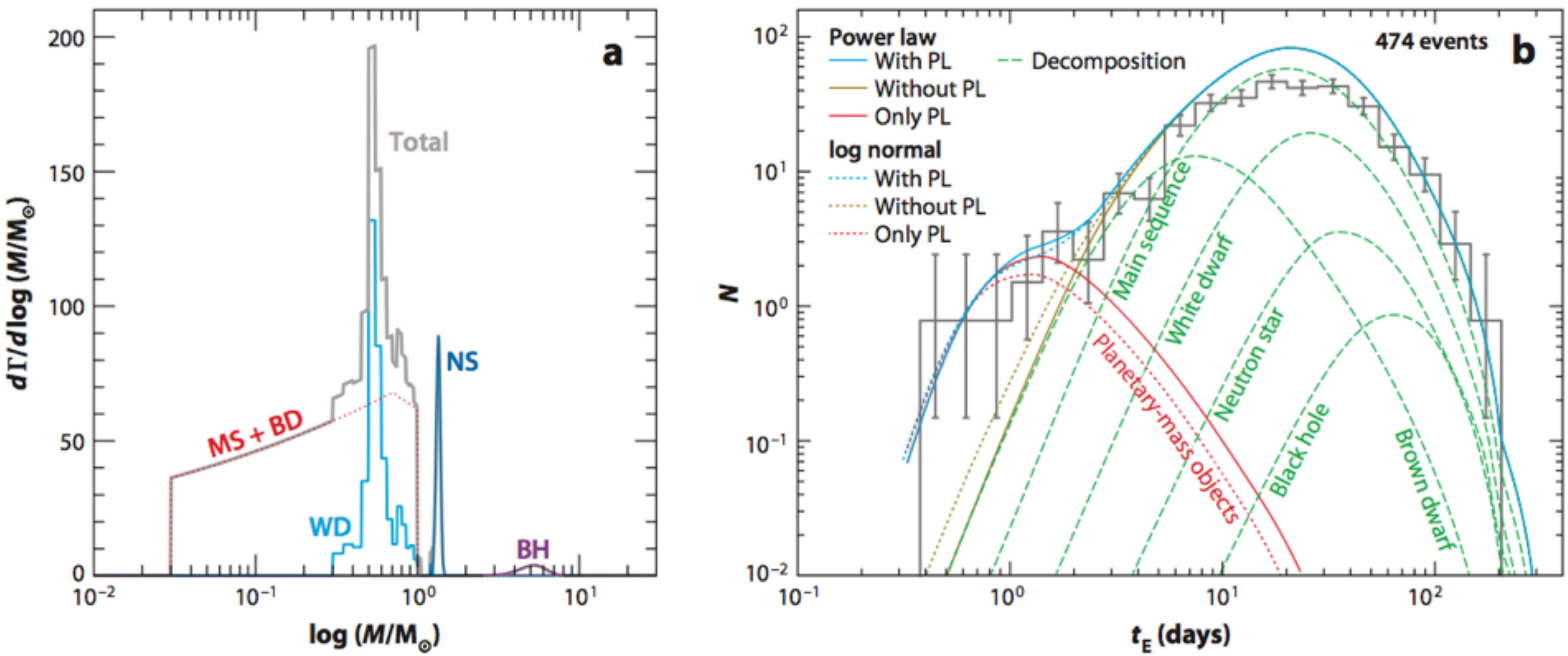
a
Total
NS
MS + BD
WD
BH
dΓ/dlog (M/M⊙)
log (M/M⊙)
b
474 events
Power law
With PL
Without PL
Only PL
Decomposition
log normal
With PL
Without PL
Only PL
Main sequence
White dwarf
Neutron star
Black hole
Brown dwarf
Planetary-mass objects
N
tE (days)

microlensing and WFIRST

WFIRST-AFTA will:

- Detect 2800 planets, with orbits from the habitable zone outward, and masses down to a few times the mass of the Moon.
- Be sensitive to analogs of all the solar system's planets except Mercury.
- Measure the abundance of free-floating planets in the Galaxy with masses down to the mass of Mars

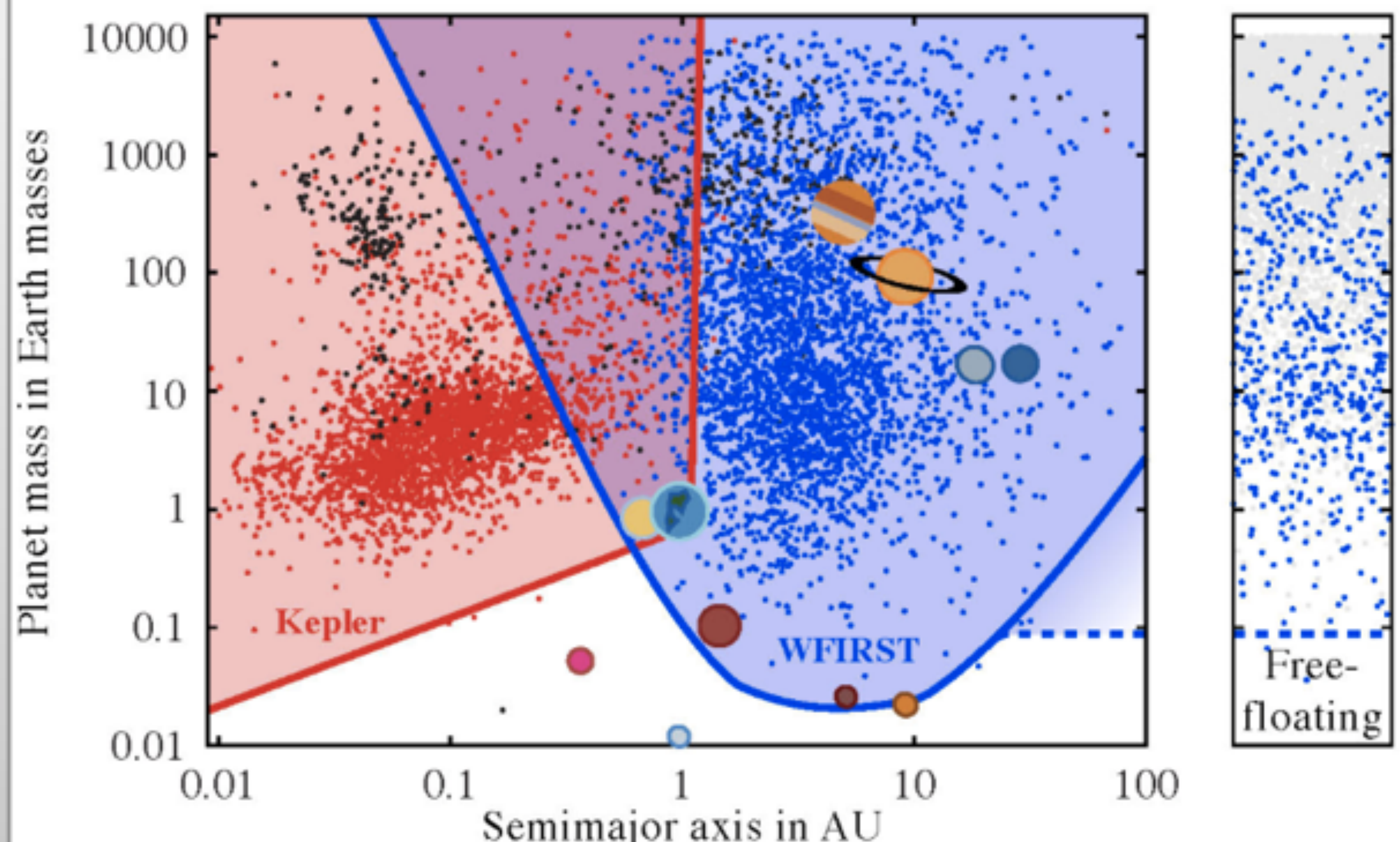

Bennett + NASA

Finite Source Effects & Microlensing Parallax Yield Lens System Mass

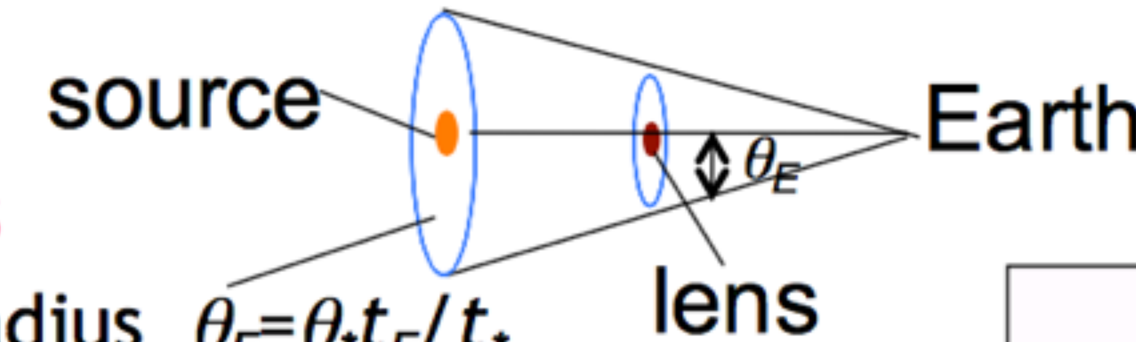

- Finite source effects

  Angular Einstein radius $\theta_E = \theta_* t_E / t_*$

  θ_* = source star angular radius

  D_L and D_S are the lens and source distances

$$M_L = \frac{c^2}{4G}\theta_E^2 \frac{D_S D_L}{D_S - D_L}$$

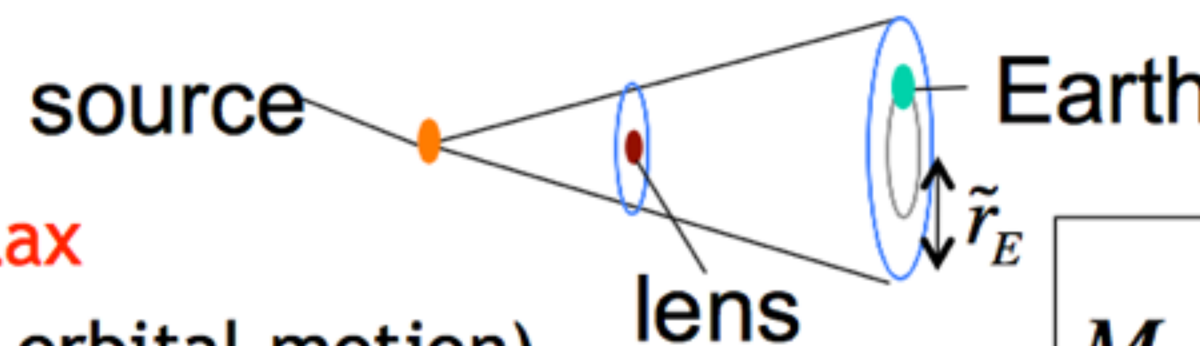

- Microlensing Parallax

  (Effect of Earth's orbital motion)

  Einstein radius projected to Observer $\tilde{r}_E$

$$M_L = \frac{c^2}{4G}\tilde{r}_E^2 \frac{D_S - D_L}{D_S D_L}$$

OR

- One of above +

  Lens brightness & color(AO,HST)

  mass-distance relation ➔ D_L

$$M_L = \frac{c^2}{4G}\tilde{r}_E \theta_E$$

Bennett + NASA

microlensing and WFIRST

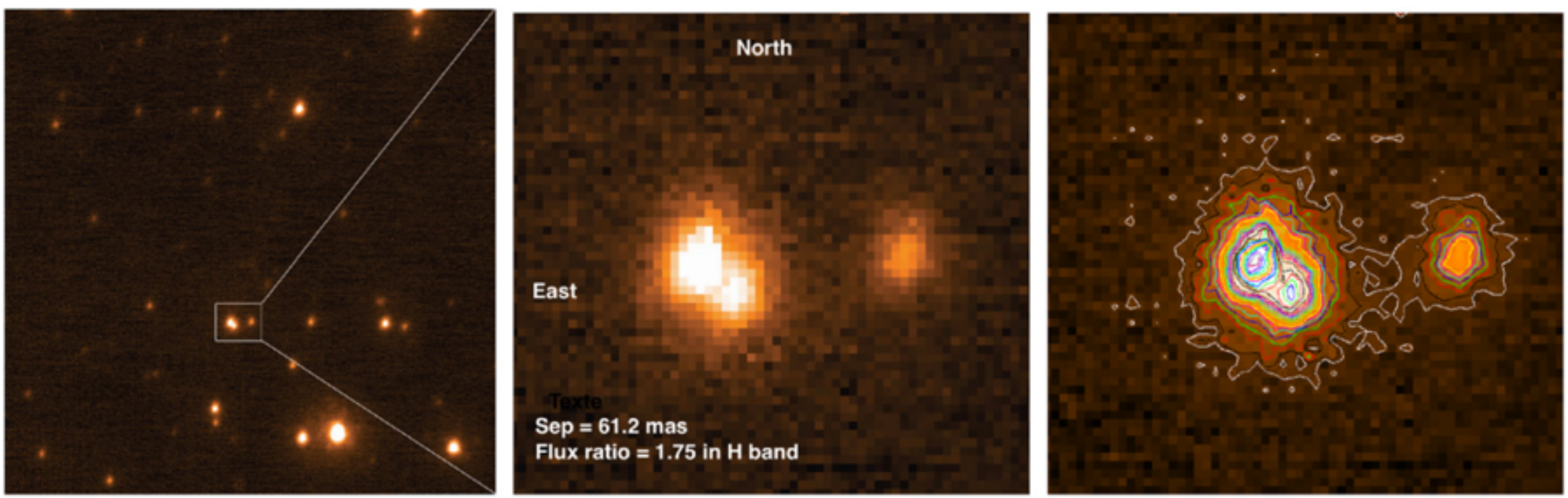

Figure 3. Left: Keck image of OGLE-2005-BLG-169 in H band ($\sim 24'' \times 21''$). Middle: a zoom on the target showing the lens on the upper left and the source. They are separated by ~61 mas. The extra star on the right was part of the measured blending in the microlensing light curve. Right: zoom on the target showing the flux contours.

microlensing and WFIRST

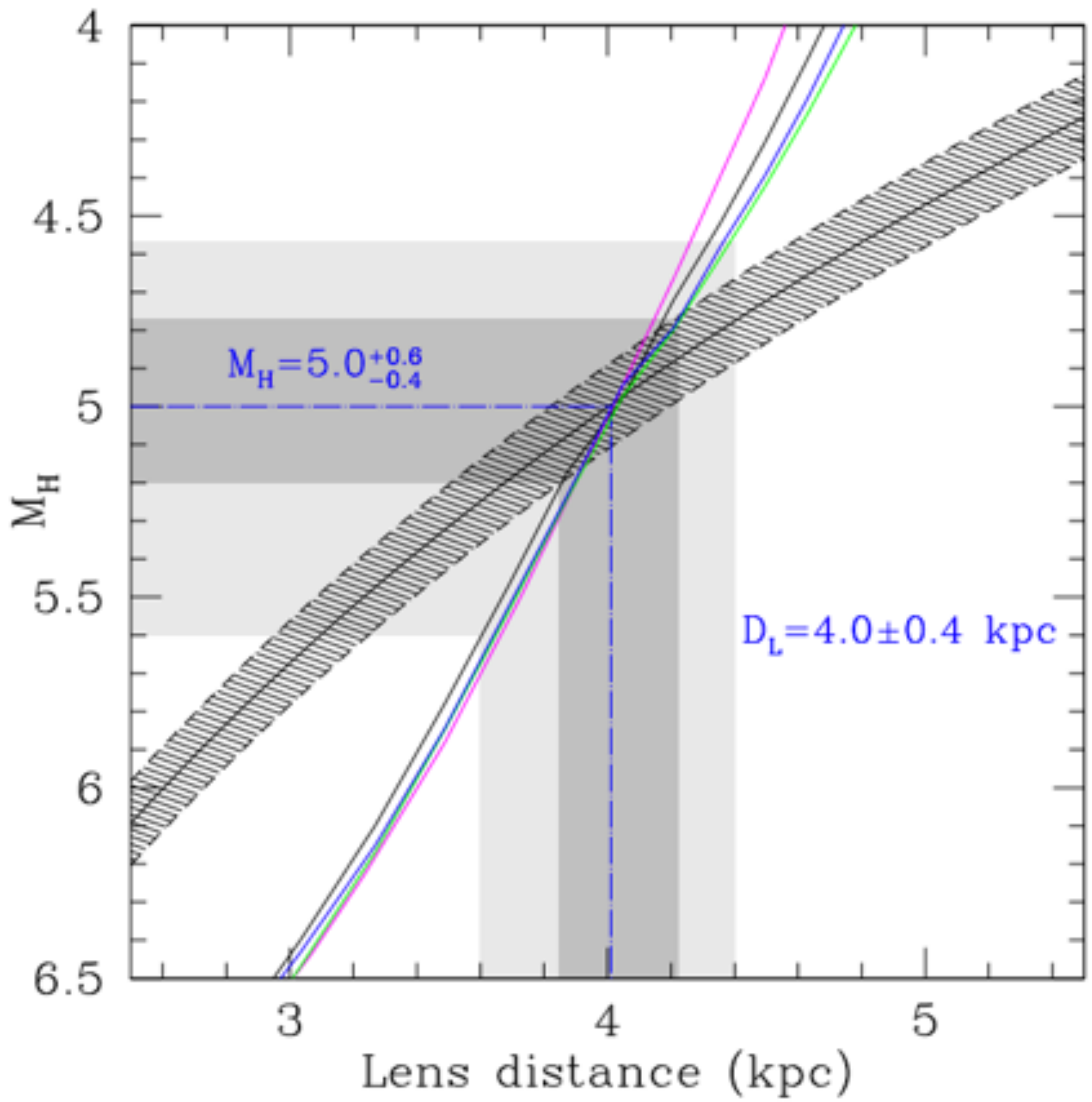

Table 1
Model Parameters from the Microlensing Light Curve

Parameter	Units	Bennett_{2015}	Gould_{2006}
t_E	days	41.8 ± 2.9	43 ± 4
θ_E	mas	0.965 ± 0.094	1.00 ± 0.22
H_S	...	18.81 ± 0.08	18.83 ± 0.09
t_*	days	0.0202 ± 0.0017	0.019 ± 0.004

distance, and the relative lens–source proper motion, $\mu_{\rm rel}$, where:

$$t_E = \frac{\theta_E}{\mu_{\rm rel,geo}}, \quad \theta_E^2 = \kappa M_L \pi_{\rm rel},$$

$$\pi_{\rm rel} = \text{AU}\left(\frac{1}{D_L} - \frac{1}{D_S}\right) \text{ and}$$

$$\kappa = \frac{4G}{c^2 \text{AU}} = 8.144 \text{ mas } M_\odot^{-1}. \quad (1)$$

$$M_H = H_L - A_H - \text{DM} = H_L - A_H - 5 \log \frac{D_L}{10 \text{ pc}}$$